UNIVERSIDAD **N**ACIONAL **A**UTÓNOMA DE **M**ÉXICO

PROGRAMA DE POSGRADO EN CIENCIAS FÍSICAS

INSTITUTO DE **C**IENCIAS **F**ÍSICAS

Scalar Field Reheating and Primordial Black Hole Formation

T E S I S

para optar por el grado de

Maestro en Ciencias (Física)

Presenta

Gabriel Karim Miranda Carrion

Cuernavaca, Morelos, Marzo 2020

Director de tesis

Dr. Juan Carlos Hidalgo Cuéllar
Instituto de Ciencias Físicas, UNAM

Miembros del jurado

Dr. Darío Núñez Zúñiga
Instituto de Ciencias Nucleares, UNAM

Dr. Josué De Santiago Sanabria
Centro de Investigación y de Estudios Avanzados, IPN

Dr. Juan Carlos Hidalgo Cuéllar
Instituto de Ciencias Físicas, UNAM

Dr. Luis Ureña López
Departamento de Física, División de Ciencias e Ingenierías, UGTO

Dr. Sébastien Mickaël Marc Fromenteau
Instituto de Ciencias Físicas, UNAM

Acknowledgements/Agradecimientos

Primero deseo expresar mis mayores agradecimientos a toda mi familia por todo su amor y apoyo incondicional que siempre me han brindando, muchos de mis logros se los debo a ustedes.
En especial a mi mamá Marlene Carrion, me van a faltar páginas para agradecerle tanto, el esfuerzo y las metas que he alcanzado, se refleja en el amor y el cariño que invierte día a día.
Mi hermano Ivan por inspirarme con su fortaleza para no decaer cuando todo parecía complicado e imposible, me enseñó ha siempre levantarme y salir adelante. Eres un gran ejemplo de valentía.
Mi papá Gabriel Miranda, por sus consejos y palabras de aliento que hicieron de mi una mejor persona y de una u otra forma me acompaña en todos mis sueños y metas.
Los quiero mucho.

Por supuesto le agradezco enormemente a mi asesor Juan Carlos Hidalgo a quien le tengo un gran respeto y admiración, gracias a su constante apoyo, conocimiento y enseñanza hoy puedo culminar este trabajo. Te agradezco que siempre compartes tus experiencias y consejos las cuales han aportado a mi formación profesional.
Así mismo les agradezco al comité tutoral Dr. Juan Carlos Degollado y Dr. Roberto Sussman por sus consejos y observaciones. Los miembros del jurado muchas gracias por tiempo y su participación e interés en evaluar este trabajo.

Mis compañeros durante la maestría y amigos de licenciatura: Brandon, Josué, Roel, Jairo, Gerson, Tapia, Andrea, Merari, Fernando, Miguel, Jazhiel, Daniel, Luis, Marco y a los que haya olvidado mencionar, les agradezco por brindarme su maravillosa amistad y apoyarme en momentos alegres y difíciles.

Me han motivado a alcanzar mis anhelos...
¡Muchas gracias a todos!

Por último, quisiera dar un agradecimiento especial al Consejo Nacional de Ciencia y Tecnología (CONACyT) por proporcionarme una beca con el fin de financiar mis estudios de posgrado.

La tesis fue redactada en el idioma inglés.

«However difficult life may seem there is always something you can do and succeed at»
Stephen Hawking

Abstract/Resumen

Reheating is a relevant cosmological epoch, since it connects the required bridge between the primordial inflationary stage and the hot big bang. On one hand, cosmological perturbations may have played an important role during the Reheating since they provide us with a valuable number of observables that characterize this stage of the Universe's evolution. On the other hand, perturbations could lead to gravitational collapse and, for large amplitude inhomogeneities, form primordial black holes (PBHs).

In this thesis, we developed both analytical and numerical study of a cosmological real and complex scalar field with no self-interaction. Specifically in the regime $H \ll \mu$, when scalar field has an oscillatory behaviour and it can also be treated as a pressure-less fluid. Afterwards we examined the case that the field represents the dominant matter; in this context, the complex scalar field may or may not be the inflaton itself. The homogeneous case is completely described by Klein-Gordon equation and initial conditions inherited by the last e-folds of inflation.

Furthermore a perturbative treatment of the scalar field fluctuations is presented where we derived the Mukhanov-Sasaki (M-S) equation and we explored the purely growing mode of these linear fluctuations. Subsequently, with the above at hand we compute the Power Spectrum of the curvature perturbations and evolve the inhomogeneities during the oscillatory phase.

We focused on constraining the abundance of PBHs formed in this period. The goal has been to impose restrictions to the model of Reheating through constraints to the Curvature Power Spectrum, at scales far smaller than those probed by cosmological observations, due to a possible overproduction of PBHs.

For instance, bounds to the PBH abundance could be employed to constrain the Curvature Power Spectrum, and hence models of inflation which estimate a Reheating period similar to that studied here.

Lastly, implications of our results and extensions to the present work are discussed in the last chapter.

Reheating es una época cosmológica relevante, ya que representa el puente requerido entre la etapa inflacionaria primordial y el hot big bang. Por un lado, las perturbaciones cosmológicas pueden haber jugado un papel importante durante el recalentamiento, ya que nos proporcionan un valioso número de observables que caracterizarían la evolución del Universo durante está época. Por otro lado, las perturbaciones podrían conducir al colapso gravitacional y, para inhomogeneidades de gran amplitud, dar lugar a la formación de agujeros negros primordiales (PBH).

En esta tesis, desarrollamos un estudio analítico y numérico de un campo escalar cosmológico real y complejo sin autointeracción. Específicamente en el régimen $H \ll \mu$, cuando el campo escalar tiene un comportamiento oscilatorio y además se puede tratar como un fluido sin presión. Examinamos el caso de que el campo representa la materia dominante durante está etapa del Universo; En este contexto, el campo escalar puede ser o no el inflatón mismo. Este caso homogéneo está completamente descrito por la ecuación de Klein-Gordon y las condiciones iniciales heredadas por los últimos e-folds de inflación.

Además, se presenta un tratamiento perturbativo de las fluctuaciones del campo escalar donde derivamos la ecuación de Mukhanov-Sasaki (M-S) y exploramos el crecimiento puramente lineal de estas perturbaciones. Posteriormente, con lo anterior en mano, procedemos a calcular el espectro de potencias de las perturbaciones de curvatura y evolucionamos las inhomogeneidades durante la fase oscilatoria.

Nos centramos en restringir la abundancia de PBH formados en esta etapa cosmológica. El objetivo ha sido imponer restricciones al modelo de Reheating mediante restricciones al espectro de curvatura, a escalas mucho más pequeña que las probadas por las observaciones cosmológicas, debido a una posible sobreproducción de PBH.

Las constricciones a la abundancia de PBH podrían emplearse para restringir el espectro de potencia de curvatura y, por lo tanto, modelos de inflación que estiman un período de Reheating similar al estudiado aquí.

Por último, las implicaciones de nuestros resultados y extensiones al presente trabajo se discuten en el último capítulo.

Contents

List of Figures

Units

Throughout this thesis we will employ natural units, where the speed of light, the Planck constant and the Boltzmann constant are set to unity, i.e.

$$c \equiv \hbar \equiv k_B \equiv 1.$$

Furthermore from Chapter 3 we will frequently make use of the reduced Planck mass defined as

$$M_{Pl}^2 \equiv \frac{\hbar c}{8\pi G} \equiv \frac{1}{8\pi G}$$

with G being Newton's constant.

Notation

We have denoted "**dot**" and "**prime**" as derivatives respect to dynamical time t, and conformal time η, respectively.

We also denote partial derivatives as $\partial_\mu A = A_{,\mu}$ and $\nabla_\mu A = A_{;\mu}$ as covariant derivatives.

Convention

Latin subscripts label i : 3D euclidean space.
Greek subscripts label μ : 4D spacetime.

Our signs convention of the metric will be $(-,+,+,+)$.

Conversions

Several conversions for natural units that we will often make use.

Planck Mass	1 M_{Pl}	$=$	2.18×10^{-8} kg
		$=$	2.435×10^{18} GeV
Planck lenght	1 ℓ_{Pl}	$=$	1.616×10^{-35} m
Electronvolt	1 eV	$=$	1.602×10^{-19} J
Parsecs	1 pc	$=$	3.261 ly
		$=$	3.085×10^{16} m
Solar Mass	1 $M_\odot$	$=$	1.989×10^{30} kg

Table 1: Conversions

Acronyms: GR (General Relativity), **CDM** (Cold Dark Matter), **FLRW** (Friedmann-Lemaître-Robertson-Walker), **CMB** (Cosmic Microwave Background), **PBHs** (Primordial Black Holes), **QFT** (Quantum Field Theory), **M-S** (Mukhanov-Sasaki).

Chapter 1

Introduction

«So much Universe, and so little time»
Terry Pratchett

The Universe may have its origin driven by quantum fluctuations, since Quantum Field Theory (QFT) predicts that vacuum is not empty but is a medium filled with fluctuating quantum fields. Many of these abstract entities are modelled through *Scalar Fields*, which give structure to the spacetime, whose symmetries and invariants have been treated traditionally to predict particles. This particles are the excitation of this field according with a certain scale of energy.

For decades cosmologists have been interested on the evolution of Scalar Field and its possible repercussions in our Universe. Several models have been proposed with one or more scalar fields associated with current paradigms in cosmology, for instance: Dark Matter (Scalar Field Dark Matter see e.g. [Matos and Urena-Lopez, 2000]), Dark Energy (quintessence see [Tsujikawa, 2013] a review), inflationary fields (inflaton), among others. The main reason is that the centerpiece model or standard cosmological model called ΛCDM presents issues in both fundamental to observational aspects that do not find a simple satisfactory solution.

One or several scalar fields could have played an important role at early times due to its quantum features. These fields would be strongly related with curvature perturbations that may be the footprint for seeds of gravitational wells, or as gravitational waves, or as black holes. For example, the fluctuations in density observed in the CMB are believed to be the imprint of the inflationary field quantum fluctuations and represent the best proof that inflation itself happened. Inflation however, requires a transition to the standard hot big bang cosmology through a process generically dubbed Reheating. During Reheating before radiation dominated era, the scalar field model starts to oscillate at the inflationary potential minimum and it behaves as a pressure-less fluid. The Reheating epoch after inflation represents an important application of Quantum Field Theory (QFT) because is speculated that provided a scenario for the origin of the elementary particles. Then particles interacted with each other up to a state of thermal equilibrium with some temperature T_r, which is called the Reheating temperature.

On the other hand, evidently the nature of dark matter is still undetermined at present day, nonetheless, recently PBHs have become more popular in cosmology due to their wide mass spectrum. PBHs are good candidates to explain the

dark matter as Planck relics remnants generated during Reheating.

In order to have a clear understanding of the cosmological phenomena relevant to this thesis, in Chapter 1 we will introduce a short description of all concepts from the General Relativity (GR) point of view which can be used as a guide.

1.1 General Relativity

The *theory of General Relativity* described and formulated by physicist Albert Einstein which is one of the most successful, beautiful and extraordinary theories in physics. Furthermore, GR achieves several predictions that have been tested through observations, such as: the exact orbits of the planets on the solar system, existence of compact objects currently as black holes [Akiyama et al., 2019] and the gravitational waves, recently observed as signals from merging black holes [Abbott et al., 2016], [Abbott et al., 2017]. More relevant to cosmology, GR predicts the components that might make up our Universe [Aghanim et al., 2018] and its geometrical shape.
In order to begin the description of GR, let us mention what was that drove and motivated Einstein to generalize the concept of gravity. Einstein was looking for a way to explain the incompatibility between Newtonian mechanics and electromagnetism. This led him to formulate the theory of SR which was published in 1905, where he was interested on the physical motion of a body in the absence of gravitational forces based on his famous SR postulates,

- The laws of physics must be identical in each reference frame, regardless of its motion.
- The speed of light will be the same in every reference frame.

Centered on this, Einstein had completely changed Newton's notion that space (length, width and depth) has always been static and time has always passed at the same speed and is absolute. Nevertheless, for Einstein's Universe, time has always been related with the space as an extra coordinate. On this unusual 4 dimensional space or better-known as *spacetime*[1], a point is defined as *event* and is denoted as x^μ and hence distance between two events is known as *interval* and is given by,

$$ds^2 = g_{\mu\nu} dx^\mu dx^\nu. \tag{1.1}$$

Where $g_{\mu\nu}$ is *metric tensor*. This further describes spacetime geometry[2]. The interval is in fact a relativistic invariant. This means that this quantity will have the same magnitude in any inertial reference frame.

Einstein questioned himself about a problem where one usually associates a mass with an object, but in fact for Einstein, the mass has 2 different interpretations: the inertial mass (that resists acceleration) and gravitational mass (produces a gravitational field). Then, he thought in a somewhat idealized problem which led him to conclude that inertial mass is identical to gravitational mass that was

[1] Spacetime is manifold 4 dimensional (lorentzian manifold) homogeneous and rigid.
[2] For instance, in SR $g_{\mu\nu} = \eta_{\mu\nu} = diag(-1, 1, 1, 1)$ is just in case of Minkowski spacetime.

called *principle of equivalence*[3]. Hence more generaly, principle of equivalence stipulates so that, in a chosen locally inertia results impossible to distinguish between physical effects due to gravity and those due to acceleration, they are equivalent!

This was Einstein's key insight and years later in 1915, Albert Einstein had formulated and published the theory of GR [Einstein, 1915]. His ideas based on mathematical foundations of manifolds and differential geometry and embodied on the well-known *Einstein field equations*:

$$G_{\mu\nu} \equiv R_{\mu\nu} - \frac{1}{2} R\, g_{\mu\nu} = \frac{8\pi G}{c^4} T_{\mu\nu}. \tag{1.2}$$

Where $G_{\mu\nu}$ is the Einstein tensor which describes the curvature of spacetime and $T_{\mu\nu}$ is the Energy-Momentum tensor for which each component describes the following,

- T^{00} - Total energy density.
- T^{0i} - Energy flux in i-direction.
- T^{i0} - Momentum density.
- T^{ij} - Momentum flux.
  - isotropic pressure when $i = j$.
  - viscous stress for $i \neq j$.

As we mentioned before, this theory generalizes the concept of gravity. The single Newtonian field equation, the Poisson equation, can be recovered at the weak field limit of the theory,

$$\nabla^2 \Phi = 4\pi G \rho. \tag{1.3}$$

This is also called the non-relativistic limit. Einstein's equations (1.2) are 10 partial differential equations for the independent components of the 4D symmetric metric tensor $g_{\mu\nu}$. Evidently, it is not possible to find a general solution but if we assume some symmetries equations are simplified.

On Riemannian geometry $R^{\gamma}_{\sigma\mu\nu}$ is the Riemann curvature tensor which is a generalization of the Gauss curvature, and also is constructed from second derivatives of metric tensor $g_{\mu\nu}$ or from derivatives of Christoffel symbols $\Gamma^{\lambda}_{\mu\nu}$:

$$R^{\gamma}_{\sigma\mu\nu} = \partial_\mu \Gamma^{\gamma}_{\nu\sigma} - \partial_\nu \Gamma^{\gamma}_{\mu\sigma} + \Gamma^{\gamma}_{\mu\lambda}\Gamma^{\lambda}_{\nu\sigma} - \Gamma^{\gamma}_{\nu\lambda}\Gamma^{\lambda}_{\mu\sigma}. \tag{1.4}$$

If the covariant derivative does not have torsion contributions, then, $\Gamma^{\lambda}_{\mu\nu} = \Gamma^{\lambda}_{\nu\mu}$. Given a metric $g_{\mu\nu}$ defined upon a manifold $\mathcal{M}$ that has been chosen with a privileged connection and without torsion such that the metric is a constant covariant, i.e. $\nabla_\mu g^{\mu\nu} = 0$, this connection is known as the Levi-Civita connection so that $\Gamma^{\lambda}_{\mu\nu}$ can be calculated as follows,

[3] In the 1950s Eötvös experiment was developed in order to measure the correlation of inertial and gravitational mass, demonstrating the coincidence between the two concepts. See [Eötvös, 2008] for a review.

$$\Gamma^{\lambda}_{\mu\nu} = \frac{1}{2} g^{\lambda\omega} \left(\partial_\nu g_{\omega\mu} + \partial_\mu g_{\omega\nu} - \partial_\omega g_{\mu\nu} \right). \tag{1.5}$$

This is called the affine connection prescription. The Riemann tensor (1.4) is used to define *Ricci tensor* just by a contraction with metric tensor as,

$$R_{\mu\nu} = R^{\gamma}_{\sigma\gamma\nu}, \tag{1.6}$$

and its trace, gives place to define *Ricci scalar*,

$$R = g^{\mu\nu} R_{\mu\nu}. \tag{1.7}$$

One property of Riemann tensor (1.4) is that meets,

$$R^{\sigma}_{\mu\nu\rho,\lambda} + R^{\sigma}_{\mu\lambda\nu,\rho} + R^{\sigma}_{\mu\nu\lambda,\nu} = 0, \tag{1.8}$$

known as *Bianchi identity*. This identity implies one more important property on GR,

$$R_{\nu\mu;\nu} = 0, \tag{1.9}$$

Hence, through Einstein's equations (1.2) we obtain,

$$\nabla_\nu T^{\mu\nu} = T^{\mu\nu}{}_{;\nu} = 0, \tag{1.10}$$

the *conservation of the Energy-Momentum tensor*.

According to the calculus of variations, finding extrema in an action which is parameterized with respect to a affine parameter λ yields

$$S = \int \sqrt{g_{\mu\nu} \frac{dx^\mu}{d\lambda} \frac{dx^\nu}{d\lambda}} d\lambda. \tag{1.11}$$

Maximizing the action one recovers the *geodesic equation*, which describes the dynamics of the free particles

$$u^\mu u^\nu{}_{;\mu} = 0. \qquad \Longleftrightarrow \qquad \frac{du^\mu}{d\tau} + \Gamma^{\mu}_{\alpha\beta} u^\alpha u^\beta = 0. \tag{1.12}$$

The interesting thing about this equation is that describes trajectories of particles in free fall[4], and in particular, for mass-less particles, i.e. $ds^2 = 0$ it is only satisfied for events with velocity c or null 4-vectors.

If the trajectories are restricted on surfaces of t = const. in such a case, it is helpful to define the normal vector n^μ proportional as:

$$n^\mu \propto -g^{\mu\nu} \frac{\partial \eta}{\partial x^\nu}. \tag{1.13}$$

Here η is the conformal time which will be defined later. The vector of (1.13) is subject to the normalization constraint,

$$n^\mu n_\mu = 1. \tag{1.14}$$

Some important features of the theory of GR are,

[4]The concept of free fall is particles in free motion (no accelerated) or test particles in RG.

- Spacetime is a Lorentzian manifold equipped with a Levi-Civita connection.
- Free particles will follow null geodesics (time-like geodesics).
- Energy-Momentum tensor will always be described by a symmetric tensor such that $\nabla_\mu T^{\mu\nu} = 0$.
- Curvature of the spacetime is strongly related with matter through the Einstein's equations (1.2).

The equations of GR allow us to study the Universe as a whole. Einstein himself did it, he thought that Universe has always been static and eternal, but unfortunately his solutions were unstable and collapsed due to gravitational interaction.

In order to achieve an unchanging Universe, Einstein introduced in his equations a constant whose unique function was to keep and enhance his stable Universe model according to his belief. He named it the *cosmological constant*.

$$G_{\mu\nu} + \Lambda g_{\mu\nu} = R_{\mu\nu} - \frac{1}{2}Rg_{\mu\nu} + \Lambda g_{\mu\nu} = \frac{8\pi G}{c^4}T_{\mu\nu}. \tag{1.15}$$

It was in 1927 that Georges Lemaître[5] who was a pioneer in proposing the expansion of the Universe. He obtained an explanation of expansion with the observation of redshifted galaxies. His results did not have any special impact initially. Years later, Einstein acknowledged Lemaître's work and said that the cosmological constant had been the worst mistake of his whole life but perhaps it was not a mistake after all.

Several standard textbooks on GR are [Carroll, 2004], [Poisson, 2002], [Schutz, 2009], [Hartle, 2003] and [Misner et al., 2017] in spite of this book may not be considered the best introductory text (one may need many cups of coffee to read it) but it has a vast content.

1.2 Scalar Fields

In QFT a scalar field ϕ is usually considered, for instance, as a boson with spin equal 0 and is a quantity thoroughly defined on spacetime. In classical field theory the scalar field is the simplest kind of matter that has the property of invariance under rotations and Lorentz boosts.

One of the main motivations to develop QFT is to unify quantum mechanics with SR. From the action for a canonical and relativistic form of matter which is coupling minimally to gravity,

$$S_m[\phi] = \int dx^4 \sqrt{-g}\,\mathcal{L}\,. \tag{1.16}$$

$\mathcal{L}$ being the Lagrangian. From action variation one would derive,

$$T_{\mu\nu} = -2\frac{\partial \mathcal{L}}{\partial g^{\mu\nu}} + g_{\mu\nu}\mathcal{L}. \tag{1.17}$$

[5] Lemaître had proposed the known Big Bang theory, which he called *hypothesis of the primal atom* as the origin of the Universe.

The canonical Lagrangian for a scalar field is defined as,

$$\mathcal{L} = \frac{1}{2} g^{\mu\nu} \partial_\mu \phi \partial_\nu \phi - V(\phi). \tag{1.18}$$

The dynamics of the scalar field is governed by this Lagrangian. The first term we easily identify as kinetic energy of the scalar field and second term is the interaction potential. Explicitly, the Energy-Momentum tensor derived from (1.17) with the previous Lagrangian (1.16) is,

$$T_{\mu\nu} = \partial_\mu \phi \partial_\nu \phi - g_{\mu\nu} \mathcal{L}. \tag{1.19}$$

Thus, through (1.10) we find the *Klein-Gordon equation*,

$$\Box \phi + \frac{dV}{d\phi} = 0. \tag{1.20}$$

Where $\Box = g^{\mu\nu} \nabla_\mu \nabla_\nu$ is the d'Alembert operator[6].

We are aiming for a description of a massive complex scalar field. A convenient way to describe a complex scalar field of mass μ is by a superposition of real and imaginary part as independent real scalar fields ϕ_a and ϕ_b of mass μ, i.e. it can be written,

$$\phi = \frac{1}{\sqrt{2}} \left(\phi_a \pm i \phi_b \right). \tag{1.21}$$

and whose dynamic is defined by the real Lagrangian,

$$\mathcal{L} = \partial^\alpha \phi \partial_\alpha \phi^* - V. \tag{1.22}$$

Then using (1.17), the Energy-Momentum tensor is given as,

$$T_{\mu\nu} = \partial_\mu \phi^* \partial_\nu \phi + \partial_\mu \phi \partial_\nu \phi^* - g_{\mu\nu} \mathcal{L}. \tag{1.23}$$

Which satisfies the Klein–Gordon equation as well,

$$\Box \phi + \frac{dV}{d\phi^*} = 0. \tag{1.24}$$

For our purposes it is useful to define and use the following expressions. The scalar field density,

$$\rho \equiv n^\mu n^\nu T_{\mu\nu}, \tag{1.25}$$

where n^μ has been defined in Eq (1.13) and the isotropic pressure,

$$P \equiv T^\theta_\theta. \tag{1.26}$$

Two important points to keep in mind on the scalar field are:

- These entities are not the particles. The scalar field is an abstract entity that has the property of curving spacetime.
- Particles of this field are the quantum excitations of the scalar field.

[6]The Klein-Gordon equation for a massive scalar field is also the relativistic form of the Schrödinger equation.

The idea of QFT is adapting and describing a quantum particle as the oscillation of an abstract field. More relevantly for our subject the scalar field has important applications in our understanding of the Universe. In the next section we will briefly mention a few.

1.3 Cosmology

Cosmology has been changing through the decades, as a result meticulous examination of information about the structure, origin and evolution of the Universe provided by technological advances in telescopes and space satellites such as COBE and WMAP, and more recently the Planck satellite, and galaxy surveys like e-Boss and Boss. This gives way to future experiments that will be developed in the coming years such as DESI, Euclid, Pixie, LiteBIRD and among others.
Our deepest understanding of the Universe is captured by a simple, elegant concept — the standard model of cosmology often called ΛCDM, which is also the most supported by observations. Today, we know in fact that the observations indicate that the Universe is mainly composed just by 3 components; matter (mostly dark matter), radiation and domination by the enigmatic dark energy as shown in Figure 1.1. Although, our current lack of understanding about the nature dark energy and dark matter gives room to more speculative models and concepts that continue to attract attention in cosmologists community.

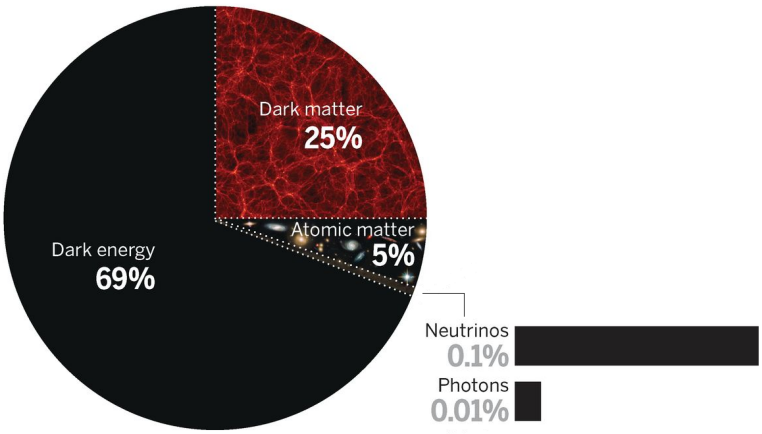

Figure 1.1: Image courtesy from [Spergel, 2015]

At the beginning of the last century, we had little idea of how the Universe was formed or what it was made of, how it has evolved and what will be its future. The key question has always been "How does the Universe work?".

We thought that the Universe originated in a classic big bang which stipulates that perhaps at the origin, all matter initially was contained within a tiny space at an extraordinarily high density and temperature.

The identification of anisotropies on the ~ 3K microwave background, the distribution of matter in the form of galaxies, and the Universe expansion are perhaps the most successful insights of the classical theory, yet the same observations that confirm the features of this theory, indicate the necessity of new ingredients, both inflation and the current acceleration of the Universe, these post open questions to modern cosmology.

Good introductory textbooks on Modern Cosmology are [Dodelson, 2003] and [Lyth and Liddle, 2009].

Cosmic Microwave Background

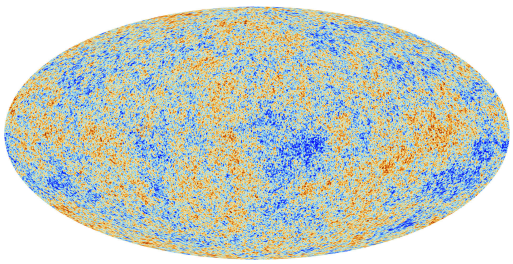

Figure 1.2: The CMB anisotropies of temperature measured by Planck with an average temperature of 2.7 K.

The Cosmic Microwave Background (CMB) is the oldest snapshot that we have been able to observe as yet. It has the early Universe footprint, as a tenuous radiation that fills the Universe. Such radiation reaches the Earth from every direction with an almost uniform intensity. CMB is a relic which shows the state of our Universe when the photons ceased scattering hydrogen atoms and were released at the epoch of recombination when the Universe was $\sim 300,000$ years old at a temperature of about $3,000$ K.

The residual radiation is extremely important for cosmologists in order to analyze a pattern of tiny variations on temperature that are better-known as anisotropies of the CMB (see Figure 1.2). After several decades of searching, CMB anisotropies were detected and mapped over a range of angular scales and ℓ-modes, so that cosmological parameters can be estimated.

Cosmological principle

The most important and fundamental assumption on Cosmology is: *The Cosmological principle*, which states that for scales sufficiently large (at least 100-150 Mpc) the distribution of the large cosmic structure ought to be statistically isotropic and homogeneous. Our picture of the CMB is consistent with such principle.

In the 1920s Hubble realized that farther galaxies are moving faster and faster away from us. During his work measuring the distances to a sample of galaxies, he showed that the distance to a galaxy and the recessional velocity are directly correlated and are given according with Hubble–Lemaître law,

$$v_H = Hr, \qquad r \quad \text{is the physical radius.} \tag{1.27}$$

With H being the rate of expansion or often called as *Hubble parameter*. Hubble estimated the value of the expansion factor, to be around 500 km/s/Mpc. Decades later Adam Riess provided evidence that the expansion of the Universe is accelerated[7].

[7]Nevertheless, nowadays cosmologists are engaged in a tremendous discussion about the expansion of the Universe due to H_0 value is still rather discrepancy (see [Riess, 2019] a short

Redshift

Relativistic Doppler effect provide an important definition of distances due to cosmic expansion. The *redshift*, which is the separation distance between the observable λ_0 and emitted λ_e wavelength is defined as,

$$z \equiv \frac{\lambda_0 - \lambda_e}{\lambda_e}. \tag{1.28}$$

Whereas electromagnetic waves move further away from us, they elongate and shift into lower frequencies.

1.3.1 Friedmann-Lemaître-Robertson-Walker solution

Between the years 1922 - 1924 the Friedmann-Lemaître-Robertson-Walker (FLRW) solution to Einstein's equations (1.2) was implemented. This exact solution is built under the assumption of the *Cosmological Principle*. Such solution provides descriptions of particular sets of Universes that can be governed by several ingredients; for example, matter, dark energy, curvature or radiation. Depending on their energy contributions, a Universe compatible with our observatons can be formulated, an analogy is like identifying a suspect with his fingerprint.

Interestingly, the most important feature of these solutions was that a static Universe is impossible: the Universe must be on expanding or contracting depending of what type of matter distribution conforms it, and therefore, the light from distant objects must be redshifted or blueshifted accordingly. The main assumption for these solutions is the cosmological principle. Generally, the FLRW metric is written in spherical coordinates as,

$$ds^2 = -c^2dt^2 + a^2(t)\left[\frac{d\chi^2}{1 - K\chi^2} + \chi^2 d\theta^2 + \chi^2 sin^2\theta d\varphi^2\right]. \tag{1.29}$$

Where $a(t)$ is the scale factor, χ are commonly called comoving coordinates that move along with the expansion of the Universe and K is the curvature of the space. However, the sign of K could be positive (closed), negative (open) or null (flat), Figure 1.3 is describing the shape of the Universe according with K sign.

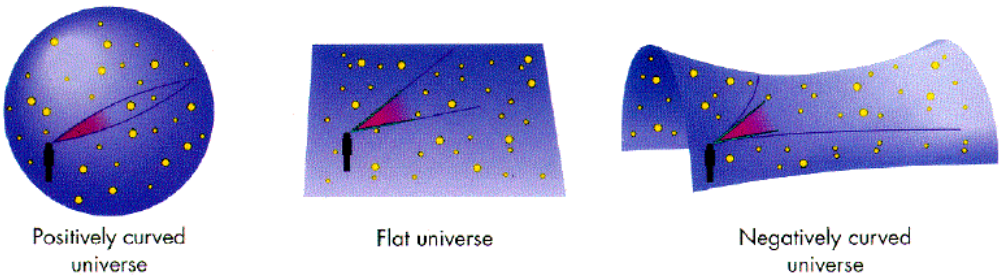

Figure 1.3: Sketch courtesy: James Schombert's UOregon 21st century science.

This leads to define H in terms of the scale factor as,

review). This tension on the H_0 value seems to depend on whether the measurements are based on the early Universe or today. We just mention this tension as part of modern cosmology but we will not go into detail because it is not related to this work.

$$H \equiv \frac{\dot{a}}{a}, \tag{1.30}$$

and,

$$q \equiv -\frac{\ddot{a}\, a}{\dot{a}^2}, \tag{1.31}$$

the deceleration rate, today with a value of $q_0 \sim 0.55$. Moreover, the scale factor can be rewritten in terms of z redshift,

$$a = \frac{a_0}{1+z}. \tag{1.32}$$

This is a useful expression in cosmology, where a_0 is the scale factor at today[8].

As for the properties of components of this Universe, an isotropic perfect fluid is often used to describe several of the constituents. The cosmological principle forces the macroscopic velocity to be isotropic. Therefore, the 4-velocity only has one temporal component,

$$u^\mu = (c, 0, 0, 0). \tag{1.33}$$

As a result, the energy-momentum tensor for a perfect fluid is given by,

$$T_{\mu\nu} = \left(\rho + \frac{P}{c^2}\right) u_\mu u_\nu + P g_{\mu\nu}. \tag{1.34}$$

Friedmann equations

Let us proceed to derive the Friedmann equations from Einstein's field equations with a cosmological constant. First of all, if we want to derive Friedmann equations, we would calculate the Christofell symbols given by (1.5) through the metric tensor $g_{\mu\nu}$ of (1.29). Fortunately the metric tensor $g_{\mu\nu}$ is diagonal and due to the symmetry of Christofell symbols several are null. Once obtained the non-zero Christofell symbols, we are able to calculate the components of Ricci tensor from (1.6). The temporal component is,

$$R_{tt} = -\frac{3}{c^2}\frac{\ddot{a}}{a}. \tag{1.35}$$

And the spatial components are,

$$R_{\chi\chi} = \frac{a\ \ddot{a}}{c^2(1-K\chi^2)} + \frac{2\dot{a}^2}{c^2(1-K\chi^2)} + \frac{2}{K(1-K\chi^2)}. \tag{1.36}$$

$$R_{\theta\theta} = \frac{\chi^2 a\ \ddot{a}}{c^2} + \frac{2\chi^2\dot{a}^2}{c^2} + 2K\chi^2. \tag{1.37}$$

$$R_{\varphi\varphi} = \frac{\chi^2 a\ \ddot{a}\ sin^2\theta}{c^2} + \frac{2\chi^2\dot{a}^2 sin^2\theta}{c^2} + 2K\chi^2 sin^2\theta. \tag{1.38}$$

Also it can be seen that Ricci tensor is diagonal, so that we could rewrite the spacial component as,

$$R_{ij} = \frac{g^{ij}}{c^2\ a^2}\left(a\ \ddot{a} + 2\dot{a}^2 + 2Kc^2\right). \tag{1.39}$$

[8] Often is setting as $a_0 = 1$.

Finally, obtaining the Ricci scalar from (1.7),

$$R = -\frac{6}{c^2}\frac{\ddot{a}}{a} - \frac{6}{c^2}\left(\frac{\dot{a}}{a}\right)^2 - 6\frac{K}{a^2}. \tag{1.40}$$

The temporal component of Einstein equations,

$$-\frac{3}{c^2}\frac{\ddot{a}}{a} - \frac{1}{2}\left(-\frac{6}{c^2}\frac{\ddot{a}}{a} - \frac{6}{c^2}\left(\frac{\dot{a}}{a}\right)^2 - 6\frac{k}{a^2}\right) - \Lambda = \frac{8\pi G}{c^4}c^2\rho. \tag{1.41}$$

And a single spatial component,

$$\begin{aligned}\frac{1}{c^2\,a^2}\left(a\,\ddot{a} + 2\dot{a}^2 + 2kc^2\right) - \frac{1}{2}\left(-\frac{6}{c^2}\frac{\ddot{a}}{a} - \frac{6}{c^2}\left(\frac{\dot{a}}{a}\right)^2 - 6\frac{K}{a^2}\right) + \Lambda \\ = \frac{8\pi G}{c^2}P.\end{aligned} \tag{1.42}$$

Sorting the temporal component (1.41) we arrive at,

$$H^2 = \left(\frac{\dot{a}}{a}\right)^2 = \frac{8\pi G}{3}\rho + \frac{\Lambda c^2}{3} - \frac{Kc^2}{a^2}. \qquad \text{Friedmann Equation.} \tag{1.43}$$

while for the spatial component (1.42) we obtain,

$$3\frac{\ddot{a}}{a} = -4\pi G\left(\rho + \frac{3P}{c^2}\right) + \frac{\Lambda c^2}{3}. \qquad \text{Raychaudhuri Equation.} \tag{1.44}$$

These are the Friedmann equations in a general form for a perfect fluid. This set of equations has often been used in cosmology to describe and forecast the dynamics of our Universe within the context of GR. With the above at hand, we also can combine both equations (1.43) and (1.44), and obtain the matter conservation equation or mostly known as continuity equation,

$$\dot{\rho} = -3H\left(\rho + \frac{P}{c^2}\right). \tag{1.45}$$

Although, there is another way to derive the conservation equation which is by property (1.10). In order to describe our Universe it is necessary to know its components. One problem is that we only have two independent equations for three variables to solve. Cosmologists often assume a perfect fluid endowed with a barotropic state equation as,

$$P = P(\rho) = \omega\, c^2\rho. \tag{1.46}$$

Here ω is a constant which characterizes the type of fluid/component. If we substitute (1.46) in (1.45) and solve it, we obtain

$$\rho = \rho_0\left(\frac{a}{a_0}\right)^{-3(1+\omega)}. \tag{1.47}$$

This expression define the evolution of cosmological components for each ω.

1.3.2 Cosmological components in our Universe

The generally assumed energy components to describe our Universe are matter (baryons and CDM), radiation (photons, neutrinos or another relativistic particle), dark energy and curvature.
It is quite useful to define here the critical energy density ρ_{cr}, which is the density the Universe would have in a flat space, i.e. $K = 0$. It is directly related to the expansion rate of the Universe, H by one of the Friedmann equations (1.43),

$$\rho_{cr} \equiv \frac{3H^2}{8\pi G}. \tag{1.48}$$

It is common to quote the energy density of different cosmological components in the present relative to this critical density,

$$\Omega_i \equiv \frac{\rho_i}{\rho_{cr}}, \tag{1.49}$$

where i represents any energy component. The curvature and the dark energy densities can also be defined as fractions of the critical density.

Matter

Considering that matter particles do not have any elastic collision, they are non-relativistic particles and essentially pressure-less.

$$P_m = 0, \quad \Rightarrow \quad \omega = 0. \tag{1.50}$$

Therefore,

$$\rho_m = \rho_{m,0} \left(\frac{a}{a_0} \right)^{-3}. \tag{1.51}$$

This type of matter is known as dust or pressure-less fluid. In fact, the observations and several models are suggesting that this is how dark matter behaves.

Radiation

Providing that statistical physics provides a description of a gas of photons, for instance, as an assemble of bosons with an energy $\varepsilon_i = \hbar\omega_i$, then the state equation for radiation fluid case can be expressed as,

$$P_{rad} = \frac{1}{3} c^2 \langle \rho \rangle, \quad \Rightarrow \quad \omega = \frac{1}{3}. \tag{1.52}$$

The density of radiation fluid hence evolves as,

$$\rho_{rad} = \rho_{r,0} \left(\frac{a}{a_0} \right)^{-4}. \tag{1.53}$$

Dark energy

One of the biggest problems in contemporary cosmology is the origin of the accelerated expansion of the Universe. This acceleration is often attributed to the cosmological constant. It has a constant density that permeates all the Universe.

$$\rho_\Lambda = \text{constant} \propto a^0. \tag{1.54}$$

Then comparing with (1.47), implies that $\omega = -1$,

$$P_\Lambda = -c^2\rho, \quad \Rightarrow \quad \omega = -1. \tag{1.55}$$

In particular this cosmological component is well-known as dark energy. However, as we mentioned before according with ΛCDM model and observational data, they suggest that we live in a fairly flat Universe its curvature has very low value, i.e. $k \approx 0$. We would like to construct the next table which shows how relevant quantities will evolve depending on the dominating type of energy,

	Matter	Radiation	Λ	Curvature
$\rho(t)$	$\sim a^{-3}$	$\sim a^{-4}$	const.	$\sim a^{-2}$
$a(t)$	$\sim t^{\frac{2}{3}}$	$\sim t^{\frac{1}{2}}$	$\sim \exp(H_0 t)$	$\sim t$
$H(t)$	$\frac{2}{3t}$	$\frac{1}{2t}$	H_0	$\frac{1}{t}$

Table 1.1: Evolution of relevant quantities in a Universe dominated by each of the featured cosmological components.

In order to be more accurately the standard cosmology is trying to figure out the evolution of the Universe based upon three principal components that constitutes its whole energy density. Furthermore the history of the Universe is classified on periods at which distinct components of energy dominated the energy budget. We can distinguish at least three stages of the Universe as Figure 1.4 shows, These are dubbed as matter-dominated, radiation-dominated, and dark energy-dominated periods.

1.3.3 Comoving coordinates

In general, the distance between any two points may be written as $r = a(t)\chi$, where χ is referred to as the comoving distance, r is simply the physical distance between the two points. The comoving distance is then always equal to the physical distance at the present moment in time. This and the conformal time are definitions used throughout this thesis, and it is convenient to define them before our analysis.

Conformal Time

Conformal time η, is often of practical use instead of the ordinary dynamical time t. They are both related by,

$$d\eta \equiv \frac{dt}{a(t)}. \tag{1.56}$$

It allows us to define an important quantity, the conformal Hubble parameter,

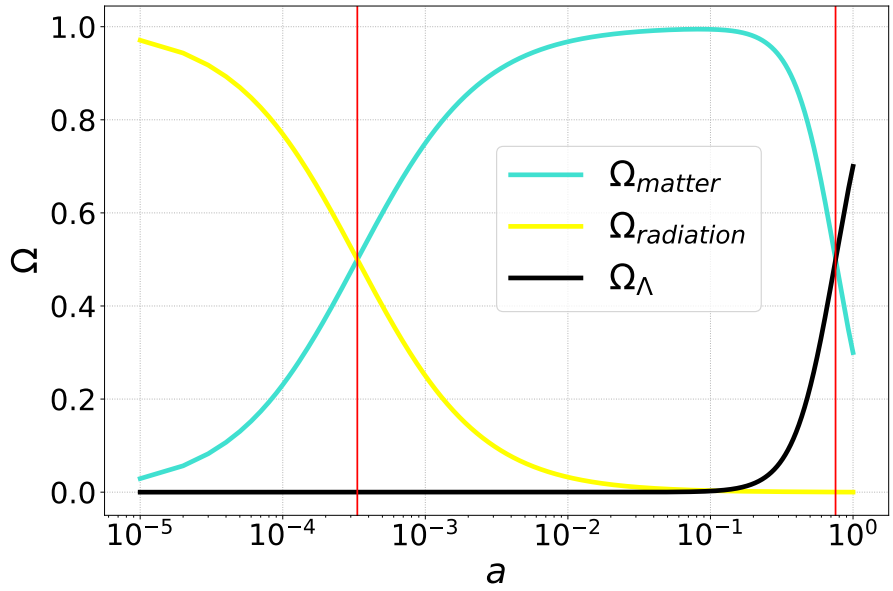

Figure 1.4: The reds lines mean the epochs of equivalence between *radiation-matter* and Λ-*matter* respectively.

$$\mathcal{H} \equiv aH. \tag{1.57}$$

The we note that the spatially flat $K = 0$ FLRW metric, given by Eq. (1.29), can be reexpressed in terms of conformal quantities as,

$$ds^2 = a^2(t)\left(-c^2 d\eta^2 + d\chi^2 + \chi^2 d\Omega^2\right) \tag{1.58}$$

In these coordinates one may then calculate the particle horizon, which is simply the maximum distance light could have travelled from the beginning, in other words, considering only radial motion (so that dropping the $d\Omega$ part),

$$0 = -c^2 d\eta^2 + d\chi^2. \tag{1.59}$$

Then,

$$\Rightarrow \quad d_H = c\int_{\eta_i}^{\eta_f} d\eta = c\int_{t_i}^{t_f} \frac{dt}{a(t)}. \tag{1.60}$$

Moreover, in a matter dominated era the particles horizon is,

$$d_H \sim 3ct, \tag{1.61}$$

and is close to the Hubble radius defined as,

$$r_H = \tfrac{3}{2} c\, t. \tag{1.62}$$

In this work we use this equivalence to identify scales above the Hubble radius, such scales are described as super-horizon.

1.4 Inflation

Inflation has been proposed as a hypothesis by the theoretical physicists Alan Guth [Guth, 1981] and Andréi Linde [Linde, 1984] in the 80s. In accordance with inflationary theory, the Universe was created in an unstable energy state, which forced a rapid expansion of the Universe at its very early moments. According with quantum theory, there is a field interpretation of inflationary theory. In this approach, the driving mechanism was due to a field generically known as *Inflaton*. In this stage the Universe expanded at least by a factor of 10^{26} and the total entropy increased likewise by a similar factor.

The inflationary theory has attempted to solve the following problems of the standard big bang cosmology[9].

1. *Flatness problem:* The initial value of Hubble parameter had to be adjusted with an exceptional accuracy (fine-tuned) to produce the practically flat Universe we observe at the present time.

2. *Horizon problem:* Stipulates that there are at least $\sim 10^{83}$ Universe regions of the observed Universe distant enough that should be causally disconnected. This means that in one Universe region the light would take more than the age of the Universe to being connected/released with another region. However, they are observed to be thermally homogeneous in average.

3. *Homogeneity problem:* The main idea for this problem is simple: Why is the Universe so incredibly uniform/homogeneous at large scales? This would require some very fine-tuned initial conditions in regions which are in principle disconnected from one another.

Inflation is a theory formulated to solve each one of these problems and more. The problem 1 can be understood from the Friedman equation (1.43) which can be rewritten as,

$$\Omega_T = 1 + \frac{K}{(aH)^2}. \tag{1.63}$$

Where Ω_T is the total density parameter and K the curvature. Actually it is easy to show that the case $K = 0$ is only a past attractor. For instance, considering a radiation epoch, energy density parameter then evolves as $(\Omega_T - 1) \sim t$. This means the curvature in the past was even flatter than the present which is constrained to be smaller than ~ 0.001.

In the inflationary theory, the Universe expanded in a way that, whatever curvature the Universe had, it was erased by the accelerated expansion[10].
The solution to the other problems listed here lies in the fact that the cosmological horizon remained constant during inflation, while the regions of the Universe in causal contact stretched beyond this horizon. Thus, after the accelerated expansion, the regions out of causal contact present common properties as observed today.

[9] Relevant textbooks are [Peter and Uzan, 2013] and Lyth and Liddle [2009], and for reviews on inflation see [Bartolo et al., 2004], [Martin, 2004].

[10] A simple analogy is when someone inflate balloon, at zooming in a region it seems almost flat.

During inflation, it is thought that other processes took place such as (see e.g. [García-Bellido]): Erasure of topological defects and magnetic monopoles, production of gravitational waves, production of non-thermal particles (as the possible origin of CDM), among others.

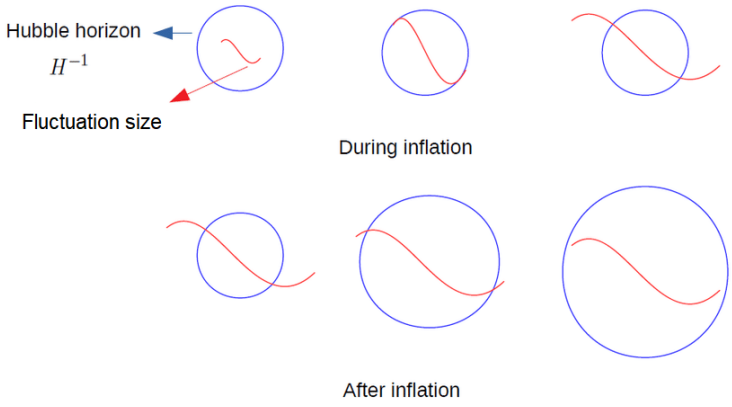

Figure 1.5: During inflation the Hubble horizon $R_H = c/H$ remains constant while the Universe is expanding and also the comoving scales exit the horizon. After inflation ends, the Universe stops accelerating and the comoving scales that were out of the horizon, begin to re-enter the horizon gradually.

The following condition must be fulfilled in order to realize inflation,

$$\text{Inflation} \quad \Leftrightarrow \quad \frac{d}{dt}\left(\frac{1}{aH}\right) < 0 \quad \Leftrightarrow \quad \ddot{a} > 0. \tag{1.64}$$

These inequality implies that the weak energy condition[11] of GR is violated,

$$\rho + 3P < 0. \tag{1.65}$$

Despite (1.65) requires negative pressure $P < -\frac{1}{3}\rho$, to be fulfilled, this results too non-intuitive. Therefore proposals or candidates that might satisfy (1.65). The scalar field ϕ seems an appropriate candidate which is better known as *Inflaton*. Indeed there are several candidates of scalar fields on cosmology such as: Curvaton, Dilaton, Phantom fields, K-essence, and even the Higgs field among others[12].

We have already defined the scalar field Lagrangian in Eq. (1.19). From this, the density and pressure are derived by expressions (1.25) and (1.26) respectively as,

$$\rho = \frac{1}{2}\dot{\phi}^2 + V(\phi) + \frac{(\nabla\phi)^2}{2a^2}. \tag{1.66}$$

$$P = \frac{1}{2}\dot{\phi}^2 - V(\phi) - \frac{(\nabla\phi)^2}{6a^2}. \tag{1.67}$$

[11] The statement of the weak energy condition is that $T^{\mu\nu}v_\mu v_\nu \geq 0$, holds for any timelike vector. In other words, the density of matter observed by a family of observers must be non-negative.

[12] Also instead of scalar fields, exists alternative theories which allows to modify GR theory them are called $f(R)$ theories (Starobinsky models).

Where $V(\phi)$ is the inflationary field interaction or in this case, the effective potential during inflation. Whether the cosmological principle and a barotropic state equation are assumed, i.e. $\phi(r,t) = \phi_0(t)$ and $P = \omega_\phi \rho$, then we would find that,

$$\underset{\text{Acceleration}}{\ddot{\phi}_0} \quad \underset{\text{Friction}}{+3H\dot{\phi}_0} = \underset{\text{Force}}{-V_{,\phi_0}}\,. \tag{1.68}$$

The homogeneous Klein-Gordon equation with an equation state,

$$\omega_\phi = \frac{\frac{1}{2}\dot{\phi}_0^2 - V(\phi_0)}{\frac{1}{2}\dot{\phi}_0^2 + V(\phi_0)}. \tag{1.69}$$

Hence for negative pressure it must satisfy that,

$$\dot{\phi}_0^2 \ll V(\phi_0). \tag{1.70}$$

On this condition the inflaton will slowly roll down through the effective potential. This period is called slow-roll, and the inequality above (1.70) is referred as the slow-roll condition.

It may be convenient to define the so-called *slow-roll parameters*[13]. They have the following expressions,

$$\epsilon_V = -\frac{8\pi G}{2}\left(\frac{V'}{V}\right). \tag{1.71}$$

This ϵ_V provides us with the slope of potential.

$$\eta_V = -\frac{V''}{V}. \tag{1.72}$$

The above is thus the curvature of potential. Additionally, $\epsilon_V \approx 1$ would establish inflation ending when potential becomes too steep and the acceleration halts.

How much inflation is enough?

The well-known *number of e-folds* N to the end of inflation is in a sense a good measure of the amount of inflation that has taken place from time t_i to t_f, and has the following definition,

$$N \equiv \int_{t_i}^{t_f} H dt = d\ln a. \tag{1.73}$$

Supposing that inflation begins at t_i and that the acceleration rate stays constant throughout inflation, $a(t) = a_i \exp(H_{inf}(t - t_i))$. The particle horizon (1.60) during inflation is,

$$d_{inf} = (a_i H_i)^{-1}\left(1 - \exp[-H_{inf}(t - t_i)]\right) \simeq (a_i H_i)^{-1}. \tag{1.74}$$

[13]Look at [Liddle et al., 1994] for more details.

Future observations

The polarization of the cosmic microwave background (CMB) or better-known as B-mode provides a direct test of inflationary model. Future missions generation such as **COrE** [Delabrouille et al., 2018], **PRISM** [André et al., 2014], **liteBIRD** [Hazumi et al., 2019] and **PIXIE** [Kogut et al., 2011] have proposed the goal to measure B modes with an unprecedented precision.

Eventually these future measurements will determine with a precision of percentage level the inflationary parameters. Therefore, tight constraints on the abundance of light elements, neutrinos, PBHs abundances and among others.

1.4.1 Reheating

After the inflationary stage, the inflaton must transfer all its energy to the rest particles of the standard model. One of the most common models for this process is a phase of oscillations of the field, which eventually couples with other matter fields through parametric oscillations (preheating). In this thesis we are concerned with the first parts of this process. This is being shown in Figure 1.6.

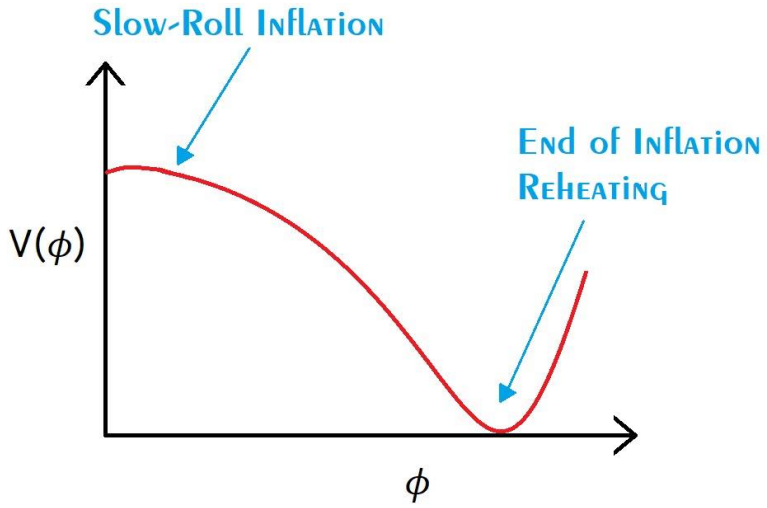

Figure 1.6: Inflationary stage is divided by two different stages. First, inflation occurs within the Slow-Roll stage, when the energy of the field is dominated by the potential $V(\phi)$, i.e, $V \gg \dot{\phi}^2$.
Secondly, after the accelerated expansion the potential $V(\phi)$ draws near to the minimum then the scalar field begins to oscillate around the minimum. This particular process is generically called Reheating.

At the last e-folds of inflation the scalar field was almost homogeneous and had an amplitude of Planck mass order $\phi \sim M_{Pl}$. While the scalar field energy is decaying and transferred through non-adiabatic way, resulting the emergence of particles for any ϕ_i-fields coupled. Given that the nature of inflation is unknown and poorly understood, this mechanism is stipulated to kickstart parametric resonance during oscillatory stage and lead to *preheating*.

Preheating is governed by non-lineal dynamics due to the coupling with other fields[14]. *Reheating* is a consequence of the parametric resonance. The decay

[14]The way in which the particle production occurs in preheating is highly model-dependent.

rate Γ_ϕ of inflation increases and eventually approaches to the expansion rate, i.e. $H \sim \Gamma_\phi$. In accordance with [Kofman et al., 1994] the decay rate could be expressed as,

$$\Gamma_\phi = \Gamma(\phi \underset{\text{Bosons}}{\rightarrow} \chi\chi) + \Gamma(\phi \underset{\text{Fermions}}{\rightarrow} \bar{\psi}\psi). \tag{1.75}$$

Where $\Gamma(\phi \rightarrow \bar{\psi}\psi) = \frac{h^2\mu}{8\pi}$ and $\Gamma(\phi \rightarrow \chi\chi) = \frac{g^4\sigma^2}{8\pi\mu}$ with σ being the minimum value of effective inflationary potential.

When the decay rate dominates over the expansion rate the Universe reaches at thermal equilibrium state or state of thermalization at a certain temperature $T_r \sim \sqrt{M_{pl}\Gamma_\phi}$. This temperature, known as *Reheating temperature* is of the order of $T_r \sim 10^{16}\ GeV$. This scale sets the end of Reheating.

During Reheating several process may arise such as: Non-perturbed effects, non-lineal interactions, processes far away from thermal equilibrium, PBH production, relics of magnetic monopole, formation solitons, q-balls or Kugelblitz, among others.

In this thesis we are going to take the simplification of about modelling the bottom of inflationary potential as Figure 1.7 shows. Hence, our simple approach will be an harmonic shape. We will take this setup as a scenario for the study of perturbations during this epoch. This thesis looks at the possible collapse of perturbations and subsequent formation of PBHs at times before the end of Reheating.

See [Peter and Uzan, 2013] or works such as [Frolov, 2010] or [Torres-Lomas et al., 2014] for more details about preheating.

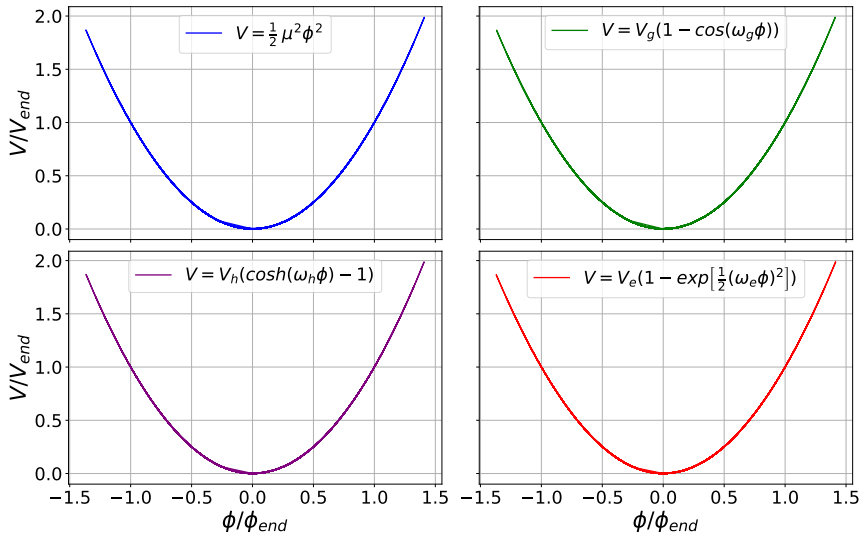

Figure 1.7: While there are several ways to generate the minimum inflationary potential, we require choosing one that is fairly consistent with the inflationary model. This plot shows a few of the models that fit a quadratic minimum, the blue was ideal potential that we will working throughout of this thesis, the green trigonometric form is an axion-like potential was developed essentially as ultralight dark matter see [Cedeño et al., 2017], while purple is a scalar field potential with a cosh-like and self-interaction have been studied by [Matos et al., 2009] and finally red also, mimics the harmonic potential, although we have not found literature studying this particular realization.

Chapter 2

Cosmological Perturbation Theory

«Everything in life is vibration»
Anonymous

Until now, we have discussed a Universe statistically homogeneous and isotropic on large scales, nevertheless that is not the Universe we live in.
The treatment at linear order in cosmological perturbation theory has been extremely useful to understand the anisotropies on the CMB detected in the microwave region of the electromagnetic spectrum. The typically values of temperature fluctuations are in order of $\sim 10^{-5}$. On the other hand, this is not the situation for matter perturbations, linear order is accurate on large scales because perturbations are in order of $\delta \ll 1$. Once one is placed on small scales the things are thoroughly different, linear order is not valid at all, due to $\delta \approx 1$. As time goes, more and more structure begins to form, so linear order becomes less and less accurate, but there has a large range of scales over which the matter fluctuations are still perturbative (and so that one does not have to run expensive simulations).

In cosmological perturbation theory the background spacetime is always the FLRW Universe meanwhile the perturbed spacetime is curved, and is not empty. This Chapter is based on the usual bibliography of perturbation theory [Malik and Wands, 2009] and textbooks [Ellis et al., 2012] and [Lachièze-Rey, 2012] as well as courses notes [Baumann, 2012] and [Kirklin, 2015] with all of these adapted to our conventions and notation.

2.1 Newtonian perturbations

For now we would like to examine a fluid in equilibrium with a density ρ without viscosity, pressure P and a velocity distribution $\vec{v}$ without vorticity sources, all of this on top of an expanding background. The gravitational interaction is mediated through to a gravitational potential Φ and is described by Poisson equation (1.3), thus, our dynamical system is given by,

$$\begin{cases} \dfrac{\partial \rho}{\partial t} + \rho \nabla \cdot \vec{v} = 0, & \text{Continuity equation.} \\ \dfrac{\partial \vec{v}}{\partial t} + (\vec{v} \cdot \nabla)\vec{v} = -\dfrac{\nabla P}{\rho} - \nabla \Phi, & \text{Euler equation.} \\ \nabla^2 \Phi = 4\pi G \rho, & \text{Poisson equation.} \end{cases} \tag{2.1}$$

We now address the following question: *Which are the necessary conditions for this fluid enclosed in a cloud to collapse?*

The central idea in a perturbed analysis; is to slightly modify each quantity by a small linear quantity, this can be expressed as,

$$\rho = \rho_0 + \delta\rho, \quad P = P_0 + \delta P, \quad \vec{v} = \vec{v}_0 + \delta\vec{v}, \quad \Phi = \Phi_0 + \delta\Phi. \tag{2.2}$$

Where ρ_0, P_0, $\vec{v}_0$, and Φ_0 are solutions of equilibrium or better known as background solutions (of the homogeneous and isotropic spacetime) and perturbations are $\frac{\delta\rho}{\rho_0}, \frac{\delta P}{P_0}, \frac{\delta\vec{v}}{\vec{v}_0}, \frac{\delta\Phi}{\Phi_0} \ll 1$.

Substituting (2.2) in (2.1) and reducing terms with the help of the background solution, we may reduce them to a perturbations dynamical system,

$$\begin{cases} \dfrac{d}{dt}\left(\dfrac{\delta\rho}{\rho_0}\right) + \nabla\cdot\delta\vec{v} = 0, \\ \dfrac{d\delta\vec{v}}{dt} + (\delta\vec{v}\cdot\nabla)\vec{v}_0 = -\dfrac{\nabla\delta P}{\rho_0} - \nabla\delta\Phi, \\ \nabla^2\delta\Phi = 4\pi G\delta\rho. \end{cases} \tag{2.3}$$

Since the background is uniformly expanding, it is convenient to change to comoving coordinates,

$$\vec{r} = a(t)\vec{x}, \qquad \vec{v} = \frac{dr}{dt} = \dot{a}\vec{x} + a\frac{dx}{dt} = \vec{v}_0 + \delta\vec{v}. \tag{2.4}$$

Furthermore setting $\vec{u} = \frac{d\vec{x}}{dt}$, the Euler equations take the next form,

$$\frac{d\vec{u}}{dt} + 2\frac{\dot{a}}{a}\vec{u} = -\frac{1}{a^2\rho_0}\nabla_c\delta P - \frac{1}{a^2}\nabla_c\delta\Phi. \tag{2.5}$$

Particularly the pressure and density perturbations could be related with an adiabatic sound speed,

$$\left(\frac{\partial P}{\partial\rho}\right)_S = c_s^2. \tag{2.6}$$

Continuity equation also has been rewritten into comoving coordinates as,

$$\frac{d}{dt}\left(\frac{\delta\rho}{\rho_0}\right) + \nabla_c\vec{u} = 0, \tag{2.7}$$

and Poisson equation too,

$$\nabla_c^2\delta\Phi = 4\pi G a^2\delta\rho, \tag{2.8}$$

where $\nabla_c = a\nabla$. Afterwards we took the divergence ∇_c to (2.5) and $\frac{d}{dt}$ of (2.7), and therefore both are combined and can be simplified with (2.8) to obtain,

$$\frac{d^2\delta}{dt^2} + 2\frac{\dot{a}}{a}\frac{d\delta}{dt} = \frac{c_s^2}{a^2}\nabla_c^2\delta + 4\pi G\rho_0\delta. \tag{2.9}$$

Here we have defined the density contrast given by,

$$\delta(x^i,t) \equiv \frac{\delta\rho}{\rho_0} = \frac{\rho(x^i,t)-\rho_0}{\rho_0}. \tag{2.10}$$

Moreover solutions of (2.9) could be expressed as a superposition of plane waves,

$$\delta(x^i,t) = \int_V \delta_{\mathbf{k}}(t)\, \exp(i\vec{k}\cdot\vec{r})\, d^3k. \tag{2.11}$$

Hence,

$$\frac{d^2\delta_{\mathbf{k}}}{dt^2} + 2H\frac{d\delta_{\mathbf{k}}}{dt} = (4\pi G\rho_0 - k^2c_s^2)\delta_{\mathbf{k}}. \tag{2.12}$$

This is called the *Jeans equation*. It is fundamental to describe the growth of structure in classic perturbations.

2.1.1 Jeans criterion

On one hand, whether the pressure dominates and reaches a value that is enough to keep supporting gravity, then density perturbations will oscillate with a decreasing amplitude (damped), this means,

$$4\pi G\rho_0 - k^2c_s^2 \leq 0. \tag{2.13}$$

On the other hand, perturbations grow exponentially when gravity pulls stronger than pressure,

$$4\pi G\rho_0 - k^2c_s^2 > 0. \tag{2.14}$$

In terms of wavelengths, we must define *Jeans scale* as,

$$\lambda_J \equiv c_s\sqrt{\frac{\pi}{G\rho_0}}. \tag{2.15}$$

In other words, density perturbations $\delta_{\mathbf{k}}$ will have two different regimes separated by a particular scale λ_J,

$$\begin{cases} \text{If} \quad \lambda > \lambda_J & \text{Growth (instability).} \\ \text{If} \quad \lambda \leq \lambda_J & \text{Oscillate (Sound waves).} \end{cases} \tag{2.16}$$

For the growing case $\lambda \gg \lambda_J$, the rate of growth is given by $(4\pi G\rho_0)^{\frac{1}{2}}$ and this allows us to define a characteristic time,

$$\tau_0 = (4\pi G\rho_0)^{-\frac{1}{2}}. \tag{2.17}$$

Actually this is the collapsing time of certain region with a density ρ_0.

Growth of Dark Matter structure

Let us now look at how inhomogeneities evolve in a matter dominated Universe, a topic relevant for the formation of Large Scale Structure (LSS). Note that the Jeans scale in this case is zero because the pressure and c_s are absent,

$$\ddot{\delta}_m + 2H\dot{\delta}_m - 4\pi G\rho_m\delta_m = 0. \tag{2.18}$$

Since $P = 0$ for a matter fluid, during the matter-dominated we have seen (see Table 1.1) how the scale factor evolves and the Hubble parameter as well. Therefore, substituting the Friedmann equation (1.43), so that (2.18) is modified as,

$$\ddot{\delta}_m + \frac{4}{3t}\dot{\delta}_m - \frac{2}{3t^2}\delta_m = 0. \tag{2.19}$$

Seeing that form of the above differential equation. We would like to suggest a polynomial solution as $\delta_m \sim t^p$. So, we found the following two solutions,

$$\delta_m \propto \begin{cases} t^{-1} \propto a^{-\frac{3}{2}} \\ t^{\frac{2}{3}} \propto a \end{cases} \tag{2.20}$$

Clearly the first solution corresponds to a decreasing mode while the second is a growing form of the fluctuations. The presence of each depends on the initial conditions. Since we are interested on the growing of structure, we have dropped out the decreasing mode. Keep in mind the growing mode of dark matter perturbation grows similar to the scale factor, $\delta_m \propto a$, during a matter-dominated epoch. This is an important result which will be discussed in the rest of this work.

2.2 Relativistic linear perturbations

Firstly, we may wonder, "Why is necessary a relativistic description for the perturbations?". Well, the short answer is, the classical perturbation is inappropriate or inadequate describing scales larger than Hubble horizon (super-horizon scales) and also for relativistic matter components like photons, neutrinos or another relativistic particle, cannot be described in a Newtonian formalism. For a rigorous description of this perturbation one must resort to the framework of GR.

Let us start by considering a small perturbation $\delta g_{\mu\nu}$ throughout FLRW conformal metric $\bar{g}_{\mu\nu}$ which represents the background[1]solution,

$$g_{\mu\nu} = \bar{g}_{\mu\nu} + \delta g_{\mu\nu}. \tag{2.21}$$

We will not go into tedious or technical calculations because is not the aim of this section. Directly we are going to define the most general form of line element perturbed in linear order where every term keeps factors of order one in all perturbative quantities as,

$$ds^2 = a(\eta)^2 \left[-(1+2\phi)d\eta^2 + 2B_i dx^i d\eta + \left[(1-2\psi)\delta_{ij} + 2E_{ij}\right] dx^i dx^j\right], \tag{2.22}$$

where ϕ, ψ are scalar functions, B_i is a 3D vector known as shift function and E_{ij} is symmetric tensor $E_{ij} = E_{ji}$, and trace-free $\delta^{ij}E_{ij} = 0$. The spatial term in square brackets is the curvature perturbation.

2.2.1 Scalar, vector, tensor decomposition

The scalar-vector-tensor (SVT) decomposition is an implement extremely powerful, what makes the SVT decomposition so successful is the fact that from

[1]In this section we have denoted the background of whichever quantity A with a bar $\bar{A}$.

Einstein field equations (1.2), the scalars, vectors and tensors, all can be treated separately at linear order, a property demonstrated by the Helmholtz Theorem. Then, the vectors are decomposed as,

$$B_i = \partial_i B + B_i^T, \tag{2.23}$$

with $\partial^i B_i^T = 0$, a transverse vector. While for tensors is,

$$E_{ij} = \partial_{\langle i}\partial_{j\rangle} E + \partial_{(i}\partial_{j)} E + E_{ij}^T. \tag{2.24}$$

Where $\partial_{\langle i}\partial_{j\rangle} E$ is the antisymmetrization of E given by,

$$\partial_{\langle i}\partial_{j\rangle} E \equiv \left(\partial_i\partial_j - \frac{1}{3}\delta_{ij}\nabla^2\right) E, \tag{2.25}$$

and $\partial_{(i}\partial_{j)} E$ is the symmetrization of E,

$$\partial_{(i}\partial_{j)} E \equiv \frac{1}{2}\left(\partial_i E_j + \partial_j E_i\right), \tag{2.26}$$

and where E_{ij}^T is a transverse and traceless tensor.

2.2.2 Orthonormal frame vector

According to [Lachièze-Rey, 2012], the metric $g_{\mu\nu}$ defines the orthonormal frames generated by a local basis tetrad,

$$g^{\alpha\beta} = \eta^{\mu\nu}(e_\mu)^\alpha (e_\nu)^\beta. \tag{2.27}$$

The $(e_\mu)^\alpha$ are called the tetrad components. The timelike $(e_0)^\mu$ can be interpreted like 4-velocity of the fluid,

$$(e_0)^\mu = \delta_0^\mu. \tag{2.28}$$

while the spacelike is,

$$(e_i)^\mu = (0, \delta_{ij}). \tag{2.29}$$

Since they are orthogonal, it is easy to normalize them. Hence the normalized timelike 4-vector at linear order,

$$(e_0)^\mu = a^{-1}(1-\phi)\delta_0^\mu, \tag{2.30}$$

and normalized spacelike at linear order,

$$(e_i)^\mu = a^{-1}[B_i\delta_0^\mu + (1+\psi)\delta_i^\mu - E_j^i\,\delta_j^\mu]. \tag{2.31}$$

2.3 Linear matter perturbations

As we did before with FLRW metric. For the case of matter here we have to perturb the Energy-Momentum tensor (1.34),

$$T_{\mu\nu} = \bar{T}_{\mu\nu} + \delta T_{\mu\nu}, \tag{2.32}$$

where the perturbation component is,

$$\delta T_{\mu\nu} = (\delta\rho + \delta P)\bar{u}_\mu\bar{u}_\nu + (\bar{\rho} + \bar{P})(\delta u_\mu \bar{u}_\nu + \bar{u}_\mu \delta u_\nu) - \delta P\delta_{\mu\nu} - \Pi_{\mu\nu}. \tag{2.33}$$

Herein $\Pi_{\mu\nu}$ being the anisotropic stress tensor. The spatial part can be chosen trace-free, $\Pi_{ij} = 0$. Without loss of generality, we also can set $\Pi_{00} = \Pi_{0i} = \Pi_{i0} = 0$. Although we will keep it for now.

The 4-velocity is subject to the constraint,

$$u_\mu u^\mu = -1, \tag{2.34}$$

with components at linear order as we have obtained before for time component,

$$u_0 = -a(1+\phi), \tag{2.35}$$

and spatial component

$$u_i = a(v_i + B_i). \tag{2.36}$$

In our case we are employing the orthonormal frame vectors on the frame of perturbations (2.32) as follows,

$$T^{\mu\nu} = (\hat{e}_\alpha)^\mu (\hat{e}_\beta)^\nu T^{\alpha\beta}. \tag{2.37}$$

Thus, we are obtaining all components at linear order,

$$T^{00} = \frac{\bar{\rho}}{a^2}\left(1 + \delta - 2\phi\right). \tag{2.38}$$

Where δ is contrast density (2.10) which has been defined previously. Moreover,

$$T^{0i} = T^{i0} = \frac{1}{a^2}\left(q^i + \bar{P}B^i\right). \tag{2.39}$$

Where q^i has been defined as,

$$q^i \equiv (\bar{\rho} + \bar{P})v^i, \tag{2.40}$$

which is the peculiar velocity of matter. Finally the spatial part of the tensor is,

$$T^{ij} = \frac{1}{a^2}\left[\bar{P}\delta^{ij} + (2\bar{P}\psi + \delta P)\delta^{ij} - 2\bar{P}E^{ij} + \Pi^{ij}\right]. \tag{2.41}$$

Nevertheless, is more frequent to work with mixed tensor components, the only reason is that allows much easier the calculations, so that the equations switch to the next simplest form,

$$T^0_0 = -\bar{\rho}\left(1 + \delta\right). \tag{2.42}$$

$$T^i_0 = -q^i. \tag{2.43}$$

$$T^0_i = (\bar{\rho} + \bar{P})B_i + q_i. \tag{2.44}$$

$$T^i_j = (\bar{P} + \delta P)\delta^i_j + \Pi^i_j. \tag{2.45}$$

2.4 Gauge transformation

In cosmology a gauge transformation[2] consists of a transformation which reflects the coordinate freedom of the mapping between a background FLRW spacetime and the "physical" inhomogeneous spacetime,

$$x^\mu \quad \longrightarrow \quad \tilde{x}^\mu \equiv x^\mu + \xi^\mu(\eta, x^i). \tag{2.46}$$

With $\xi^0 \equiv T$ and $\xi^i \equiv L^i = \partial^i L + (L^i)^T$. Hence, coordinates could be rewritten as,

$$\tilde{\eta} = \eta + T(\eta, x^i), \qquad \tilde{x}^i = x^i + L^i(\eta, x^i), \tag{2.47}$$

T and L are the *gauge functions*.

2.4.1 Gauge transformation for $g_{\mu\nu}$

Following the definition, gauge transformation applied on the perturbed metric (2.21) yields,

$$\delta\tilde{g}_{\mu\nu} = \tilde{g}_{\mu\nu} - \bar{g}_{\mu\nu}(\tilde{\eta}, \tilde{x}^i). \tag{2.48}$$

On the other hand, we ought take advantage of line element invariance,

$$ds^2 = g_{\mu\mu}dx^\mu dx^\nu = \tilde{g}_{\mu\nu}d\tilde{x}^\mu d\tilde{x}^\nu. \tag{2.49}$$

Then if we just write $dx^\alpha = \dfrac{\partial x^\alpha}{\partial \tilde{x}^\mu} d\tilde{x}^\mu$, that allows us to obtain the following expression,

$$\tilde{g}_{\mu\mu} = \frac{\partial x^\alpha}{\partial \tilde{x}^\mu}\frac{\partial x^\beta}{\partial \tilde{x}^\nu} g_{\alpha\beta}. \tag{2.50}$$

So, we employ it on (2.48) and find that,

$$\delta\tilde{g}_{\mu\nu} = \frac{\partial x^\alpha}{\partial \tilde{x}^\mu}\frac{\partial x^\beta}{\partial \tilde{x}^\nu} g_{\alpha\beta} - \bar{g}_{\mu\nu}(\tilde{\eta}, \tilde{x}^i), \tag{2.51}$$

or,

$$\delta\tilde{g}_{\mu\nu} = \frac{\partial x^\alpha}{\partial \tilde{x}^\mu}\frac{\partial x^\beta}{\partial \tilde{x}^\nu} \left[\bar{g}_{\alpha\beta}(\eta, x^i) + \delta g_{\alpha\beta}\right] - \bar{g}_{\mu\nu}(\tilde{\eta}, \tilde{x}^i). \tag{2.52}$$

Carrying a Taylor expansion of $\bar{g}_{\mu\nu}(\tilde{\eta}, \tilde{x}^i) = \bar{g}_{\mu\nu}(\eta + T,\ x^i + L^i)$, at linear order.

$$\delta\tilde{g}_{\mu\nu} = \frac{\partial x^\alpha}{\partial \tilde{x}^\mu}\frac{\partial x^\beta}{\partial \tilde{x}^\nu} \left[\bar{g}_{\alpha\beta}(\eta, x^i) + \delta g_{\alpha\beta}\right] - \bar{g}_{\mu\nu}(\eta, x^i) - T\bar{g}'_{\mu\nu} - L^i\partial_i\,\bar{g}_{\mu\nu}. \tag{2.53}$$

Hence, accommodating terms we finally obtain,

$$\delta\tilde{g}_{\mu\nu} = \frac{\partial x^\alpha}{\partial \tilde{x}^\mu}\frac{\partial x^\beta}{\partial \tilde{x}^\nu}\delta g_{\alpha\beta} + \left[\frac{\partial x^\alpha}{\partial \tilde{x}^\mu}\frac{\partial x^\beta}{\partial \tilde{x}^\nu} - \delta^\alpha_\mu\delta^\beta_\nu\right]\bar{g}_{\alpha\beta} - T\bar{g}'_{\mu\nu} - L^i\partial_i\,\bar{g}_{\mu\nu}. \tag{2.54}$$

The above expression (2.54) indicates a practical method to perform a gauge transformation of metric perturbation. The Jacobian matrix has been easily obtained as,

[2]Here we have denoted a gauge transformation of whichever quantity A with a tilde $\tilde{A}$.

$$\frac{\partial \tilde{x}^\alpha}{\partial x^\mu} = \begin{pmatrix} 1+T' & \partial_i T \\ L'^{\,i} & \delta^i_j + \partial_j L^i \end{pmatrix}. \tag{2.55}$$

Thus, the inverse of Jacobian matrix at linear order is,

$$\frac{\partial x^\alpha}{\partial \tilde{x}^\mu} = \begin{pmatrix} 1-T' & -\partial_i T \\ -L'^{\,i} & \delta^i_j - \partial_j L^i \end{pmatrix}. \tag{2.56}$$

Where α-index runs vertically and μ-index runs horizontally. We will work out the $\delta\tilde{g}_{00}$ component as an example,

$$\delta\tilde{g}_{00} = \frac{\partial x^\alpha}{\partial \tilde{x}^0}\frac{\partial x^\beta}{\partial \tilde{x}^0}\delta g_{\alpha\beta} + \left[\frac{\partial x^\alpha}{\partial \tilde{x}^0}\frac{\partial x^\beta}{\partial \tilde{x}^0} - \delta^\alpha_0\delta^\beta_0\right]\bar{g}_{\alpha\beta} - T\bar{g}'_{00} - L^i\partial_i\,\bar{g}_{00}. \tag{2.57}$$

Indeed, it may be reduced with taking into consideration only linear terms.

$$\delta\tilde{g}_{00} = -2a^2\tilde{\phi} = -2a^2\phi + 2a^2T' + 2a^2T\mathcal{H}. \tag{2.58}$$

Therefore,

$$\tilde{\phi} = \phi - T' - \mathcal{H}T. \tag{2.59}$$

In the same way we have derived the gauge transformation for ϕ, the rest of the quantities might be obtained. Then, after several calculations to the rest of components the transformations are found,

$$\tilde{\psi} = \psi + \mathcal{H}T + \frac{1}{3}\partial_i L^i. \tag{2.60}$$

$$\tilde{B}_i = B_i + \partial_i T - L'_i\,, \quad \underset{SVT}{\longrightarrow} \quad \tilde{B} = B + T - L'. \tag{2.61}$$

$$\tilde{E}_{ij} = E_{ij} - \partial_{\langle i}L_{j\rangle}\,, \quad \underset{SVT}{\longrightarrow} \quad \tilde{E} = E - L. \tag{2.62}$$

2.4.2 Gauge transformation for $T_{\mu\nu}$

Likewise the geometrical perturbations, energy-momentum tensor $T_{\mu\nu}$ is also subject to gauge transformations. We will work in the mixed form obtained before,

$$\delta\tilde{T}^\mu_\nu = \frac{\partial x^\mu}{\partial \tilde{x}^\alpha}\frac{\partial x^\beta}{\partial \tilde{x}^\nu}T^\alpha_\beta - \bar{T}^\mu_\nu(\eta + T,\, x^i + L^i). \tag{2.63}$$

Again doing a Taylor aproximation at 1st order,

$$\delta\tilde{T}^\mu_\nu = \frac{\partial x^\mu}{\partial \tilde{x}^\alpha}\frac{\partial x^\beta}{\partial \tilde{x}^\nu}\delta T^\alpha_\beta + \left[\frac{\partial x^\mu}{\partial \tilde{x}^\alpha}\frac{\partial x^\beta}{\partial \tilde{x}^\nu} - \delta^\mu_\alpha\delta^\beta_\nu\right]\bar{T}^\alpha_\beta - T\,\bar{T}'^{\,\mu}_{\ \nu} - L^i\partial_i\,\bar{T}^\mu_\nu. \tag{2.64}$$

So evaluating for each components after straightforward computation, we found,

$$\delta\tilde{\rho} = \delta\rho - T\bar{\rho}'. \tag{2.65}$$

$$\delta\tilde{P} = \delta P - T\bar{P}'. \tag{2.66}$$

$$\tilde{q}_i = q_i + (\bar{\rho} + \bar{P})L'_i, \quad \text{or} \quad \tilde{v}_i = v_i + L'_i, \quad \underset{SVT}{\longrightarrow} \quad \tilde{v} = v + L'. \tag{2.67}$$

$$\tilde{\Pi}_{ij} = \Pi_{ij} \tag{2.68}$$

Thus, the anisotropic stress tensor is a gauge-invariant quantity; a concept to be discussed further below.

2.4.3 Gauge-invariant quantities

Gauge invariance refers to the following property of some perturbations. Any quantity Q with a well defined and completely set gauge transformation $Q \to \tilde{Q}$ will be an invariant $Q = \tilde{Q}$. A few of them represents a physical observables or provide us information about them. In the following we list a few relevant gauge-invariant quantities, which will be used on the next sections.

Bardeen potentials

The original article by Bardeen [Bardeen, 1980] found a particular transformation form of perturbations,

$$\Phi \equiv \phi + \mathcal{H}(B - \dot{E}) + \dot{B} - \ddot{E}. \tag{2.69}$$

$$\Psi \equiv \psi - \mathcal{H}(B - \dot{E}) + \frac{1}{3}\nabla^2 E. \tag{2.70}$$

$$\Psi_i = \dot{E}_i - B_i \tag{2.71}$$

Any transformation to a different gauge of the perturbations on the right hand side represents no change for the combination of all terms. This happens to the scalar potentials of the perturbed metric (2.22) when the shear is absent as we shall see below.

Adiabatic fluctuations

In adiabatic perturbations all fluid perturbations are determinated by a single degree of freedom in the metric perturbations. Since canonical inflation is dominated by a single degree of freedom, inflation naturally predicts initial fluctuations which ought to be adiabatic. Energy densities of all species inherit the single degree of freedom and therefore their difference is constant (invariant). Thus,

$$\frac{\delta P_a}{\bar{\rho}_b + \bar{P}_a} - \frac{\delta P_b}{\bar{\rho}_b + \bar{P}_b}, \tag{2.72}$$

is a gauge-invariant, with a and b label species. Just in case all components are adiabatic, this equation vanishes. Otherwise, isocurvature perturbations appear and they can be expressed as the discrepancy between different components. From the equation above, thus we can define,

$$S_{ab} \equiv \frac{\delta_a}{1 + \omega_b} - \frac{\delta_a}{1 + \omega_b}. \tag{2.73}$$

Isocurvature perturbations is another gauge-invariant that corresponds to perturbations between different components. As stated above, if there was a single inflation field from primordial perturbations, i.e. $S_{ab} = 0$, for all types of species. For instance, employing a barotropic fluid, (2.72) becomes,

$$\frac{\delta_a}{1 + \omega_a} = \frac{\delta_b}{1 + \omega_b}. \tag{2.74}$$

Whether base on the case of matter and radiation fluids, we then find $\delta_r = \frac{4}{3}\delta_m$.

2.4.4 Relevant Gauges

Let us focus on the quantities relevant to this work. Hereafter we will neglect vectors and tensor, therefore to set a gauge completely we must determine L and T. Briefly, we would like to mention several different ways to fixed gauges and implications which are relevant to this thesis. In fact, observables are physical and do not depend on the gauge. Therefore, even if the starting point is not fully general, the results will be. Here is a list of them,

- **Newtonian** or **longitudinal gauge**

  This is the most popular gauge used in perturbation theory. It is extremely useful on formation and growth structure. Just choosing hypersurfaces of constant time where $\tilde{B} = 0$ and also isotropic hypersurfaces, i.e. $\tilde{E} = 0$. Then,

  $$ds^2 = a^2[-(1+2\Phi)d\eta^2 + (1-2\Psi)\delta_{ij}dx^i dx^j]. \tag{2.75}$$

  where $\Phi(R,\eta), \Psi(R,\eta)$ are Bardeen potentials which are describing the perturbations of spacetime (it can be shown that shear contributions are null in this gauge). Furthermore, we can obtain explicit forms for T and L in this gauge,

  $$L = E, \tag{2.76}$$

  and

  $$T = E' - B, \tag{2.77}$$

  as long as there is absences of anisotropic stress in most of the cases $\Psi = \Phi$.

- **Uniform density gauge**

  The gauge freedom can be set from condition on the matter perturbations. In the case of uniform density we choose $\delta\tilde{\rho} = 0$.

  $$T = \frac{\delta\rho}{\rho'} \tag{2.78}$$

  Although, we would need an additional condition in order to find a expression for L.

- **Comoving gauge**

  This is a gauge where all observers move along with the expansion flux. Only if we set $v_i = \mathbf{0}$, therefore, $\tilde{q}_i = \mathbf{0}$, implies from (2.44) there is null. Then, $\tilde{B} = 0$.

  $$L = -\int v d\eta + \text{const.} \tag{2.79}$$

  and

  $$T = v - B. \tag{2.80}$$

2.5 Linearised equations

Our task for now is linearise the perturbed Einstein equations,

$$\delta G_{\mu\nu} = 8\pi G \delta T_{\mu\nu}. \tag{2.81}$$

We will work with the Newtonian gauge (2.75). Hence, the respective Christofell symbols (1.5) computed at linear order are,

- $\Gamma^0_{00} = \mathcal{H} + \Phi'$.
- $\Gamma^0_{0i} = \Gamma^0_{i0} = \partial_i \Phi$.
- $\Gamma^i_{00} = \delta^{ij}\partial_j \Phi$.
- $\Gamma^0_{ij} = \Gamma^0_{ji} = \mathcal{H}\delta_{ij} - [\Psi' + 2\mathcal{H}(\Psi + \Phi)]\delta_{ij}$.
- $\Gamma^i_{j0} = (\mathcal{H} - \Psi')\,\delta^i_j$.
- $\Gamma^i_{jk} = \delta_{jk}\delta^{i\ell}\partial_\ell \Psi - 2\delta^i_{(j}\partial_{k)}\Psi$.

Now we can obtain Ricci tensor components at linear order,

$$R_{00} = -3\mathcal{H}' + \nabla^2\Phi + 3\mathcal{H}(\Psi' + \Phi') + 3\Psi''. \tag{2.82}$$

$$R_{0i} = 2\partial_i\Psi' + 2\mathcal{H}\partial_i\Phi. \tag{2.83}$$

$$\begin{aligned} R_{ij} = \big[&\mathcal{H}' + 2\mathcal{H}^2 - \Psi'' + \nabla^2\Psi - 2(\mathcal{H}' + 2\mathcal{H}^2)(\Psi + \Phi) \\ &-\mathcal{H}\Phi' - 5\mathcal{H}\Psi'\big]\,\delta_{ij} + \partial_i\partial_j(\Psi - \Phi). \end{aligned} \tag{2.84}$$

Also Ricci scalar at linear order,

$$\begin{aligned} R = -\frac{1}{a^2}[&-6(\mathcal{H}' + \mathcal{H}^2) + 2\nabla^2\Phi - 4\nabla^2\Psi \\ &+ 12(\mathcal{H}' + \mathcal{H}^2)\Phi + 6\Psi'' + 6\mathcal{H}(\Phi' + 3\Psi')]. \end{aligned} \tag{2.85}$$

Finally, after a several laborious calculations[3], we have derived all components of Einstein tensor (1.2) at linear order,

$$G_{00} = 3\mathcal{H}^2 + 2\nabla^2\Psi - 6\mathcal{H}\Psi'. \tag{2.86}$$

$$G_{0i} = 2\partial_i\Psi' + 2\mathcal{H}\partial_i\Phi. \tag{2.87}$$

$$\begin{aligned} G_{ij} = &[\nabla^2(\Phi - \Psi) + 2\Psi'' + 2(2\mathcal{H}' + \mathcal{H}^2)(\Psi + \Phi) + 2\mathcal{H}\Phi' \\ &+ 4\mathcal{H}\Psi']\delta_{ij} + \partial_i\partial_j(\Psi - \Phi) - (2\mathcal{H}' + \mathcal{H}^2)\delta_{ij}. \end{aligned} \tag{2.88}$$

Since we have all linearised components of matter as well as geometric. We would able to compute Einstein equations (1.2) at linear order. The 00-component is,

$$\nabla^2\Psi = 3\mathcal{H}(\Psi' + \mathcal{H}\Phi) + 4\pi G\bar{\rho}a^2\delta. \tag{2.89}$$

[3] I would like to recommend an awesome mathematical software based on Python called *SageMath* which has been used to check the results in this section, the extension *SageManifolds* that helped me computing all the relevant geometrical quantities.

the $\delta G_{0i} = 8\pi G \delta T_{0i}$ component is,

$$\Psi' + \mathcal{H}\Phi = -4\pi G(\bar{\rho} + \bar{P})v. \tag{2.90}$$

Whether (2.89) and (2.90) are combined in order to get the following,

$$\nabla^2 \Psi = 4\pi G a^2 \bar{\rho}\, \Delta. \tag{2.91}$$

With Δ being the comoving-gauge density perturbation defined as,

$$\Delta \equiv \frac{\delta\rho - 3\mathcal{H}(\bar{\rho} + \bar{P})(v + B)}{\bar{\rho}} = \delta + \frac{\bar{\rho}'}{\bar{\rho}}(v + B), \tag{2.92}$$

which is a gauge-invariant. For the spatial component, $\delta G_{ij} = 8\pi G \delta T_{ij}$.

$$\begin{aligned}[\nabla^2(\Phi - \Psi) + 2\Psi'' + 2(2\mathcal{H}' + \mathcal{H}^2)(\Psi + \Phi) + 2\mathcal{H}\Phi' + 4\mathcal{H}\Psi']\delta_{ij} \\ + \partial_i\partial_j(\Psi - \Phi) = 8\pi G a^2[(\delta P - 2\bar{P}\Psi)\delta_{ij} + \Pi_{ij}].\end{aligned} \tag{2.93}$$

So, let us take the trace-free part of (2.93),

$$\partial_{\langle i}\partial_{j\rangle}(\Psi - \Phi) = 8\pi G a^2 \Pi_{ij} \tag{2.94}$$

We had mentioned before without anisotropic stress contributions, Bardeen potentials become the same, and the Eq. (2.94) is a completely proof of that.
Trace part become as,

$$\Psi'' + \frac{1}{3}\nabla^2(\Phi - \Psi) + (2\mathcal{H}' + \mathcal{H}^2)\Phi + \mathcal{H}\Phi' + 2\mathcal{H}\Psi' = 4\pi G a^2 \delta P. \tag{2.95}$$

Futhermore we mentioned that most of cases the anisotropic stress (2.94) will not have any contribution. We thus are allowed to fix $\Psi = \Phi$. In consequence of this, pertubed Einstein equations then turn into,

$$\nabla^2\Phi - 3\mathcal{H}(\Phi' + \mathcal{H}\Phi) = 4\pi G\bar{\rho}a^2\delta. \tag{2.96}$$

$$\Phi' + \mathcal{H}\Phi = -4\pi G a^2(\bar{\rho} + \bar{P})v \tag{2.97}$$

$$\Phi'' + 3\mathcal{H}\Phi' + (2\mathcal{H}' + \mathcal{H}^2)\Phi = 4\pi G a^2 \delta P. \tag{2.98}$$

Those are typically linearised perturbed field equations.

2.5.1 Perturbed conservation equations

In order to derive the evolution equations for perturbations, we begin by computing the components of perturbed conservation Energy-Momentum tensor,

$$\nabla^\mu \delta T_{\mu\nu} = 0. \tag{2.99}$$

Through the first component $\mu = 0$, we obtain the following equation,

$$\delta\rho' + 3\mathcal{H}\left(\delta\rho + \delta P\right) - 3\Psi'\left(\bar{\rho} + \bar{P}\right) + \partial_i\, q^i = 0. \tag{2.100}$$

Each term of (2.100) are,

- $3\mathcal{H}$ $\rightarrow$ dilution due to expansion.
- Ψ' $\rightarrow$ density change by perturbations.

- $\partial_i q^i \rightarrow$ local fluid flux.

From definitions (2.10) and (2.40) so that the Eq. (2.100) has been rewritten as,

$$\delta' + \left(1 + \frac{\bar{P}}{\bar{\rho}}\right)\left(\partial_i v^i - 3\Psi'\right) + 3\mathcal{H}\left(\frac{\delta P}{\delta\rho} - \frac{\bar{P}}{\bar{\rho}}\right)\delta = 0. \tag{2.101}$$

These equations can be combined to recover the Newtonian evolution of perturbations only in the case of pressure-less matter (as in CDM case). With the above at hand we can now address the evolution of a scalar field which in principle would not be described in terms of a perfect fluid.
The Bardeen potential Ψ is only constant on super-Hubble scales.

2.6 Curvature perturbation

The next derivation has been followed from [Kirklin, 2015], however this will be adapted according our metric convention. The induced metric, γ_{ij} is just the spatial part of the line element (2.22),

$$\gamma_{ij} \equiv a^2\left[(1-2\psi)\delta_{ij} + 2E_{ij}\right]. \tag{2.102}$$

Afterwards of computed the 3-dimensional Ricci scalar[4] associated with (2.102).

$$a^2 R_{(3)} = 4\,\nabla^2\left(\psi - \frac{1}{3}\nabla^2 E\right). \tag{2.103}$$

The curvature perturbation then has been defined as,

$$\zeta \equiv \psi - \frac{1}{3}\nabla^2 E. \tag{2.104}$$

Which is often named Gauge-ready form. This is equivalent to the metric perturbation (2.22) evaluated in the uniform $\delta\tilde{\rho} = 0$ and comoving gauge $\tilde{B} = 0$ gauge as well. Unfortunately is not a gauge invariant yet. We would prefer it if it was gauge-invariant. Under a gauge transformation into (2.104),

$$\tilde{\zeta} = \tilde{\psi} - \frac{1}{3}\nabla^2\tilde{E}. \tag{2.105}$$

Making use of transformations previously calculated in (2.60) and (2.62). Since we also derived (2.65) in this gauge, the Eq. (2.105) is rewritten as follows,

$$\tilde{\zeta} = \zeta + \mathcal{H}T = \zeta + \mathcal{H}\frac{\delta\rho}{\bar{\rho}'}. \tag{2.106}$$

We can thus define the curvature perturbations in uniform density gauge as,

$$\zeta \equiv \psi - \frac{1}{3}\nabla^2 E + \mathcal{H}\frac{\delta\rho}{\bar{\rho}'}. \tag{2.107}$$

We could equally have used B and v gauge transformations (2.61) and (2.67) respectively as well to remove T and get,

$$\mathcal{R} \equiv \psi - \frac{1}{3}\nabla^2 E - \mathcal{H}(B + v). \tag{2.108}$$

[4] In the same way, *SageManifolds* has been used.

This is called the comoving curvature perturbation. There are important quantities which always are conserved on super-horizon scales for adiabatic fluctuations. Whether we do the difference between (2.107) and (2.108),

$$\mathcal{R}-\zeta=\mathcal{H}\frac{\delta\rho}{\bar{\rho}'}+\mathcal{H}(B+v)=\mathcal{H}\frac{\bar{\rho}}{\bar{\rho}'}\left[\frac{\delta\rho}{\bar{\rho}}+\frac{\bar{\rho}'}{\bar{\rho}}(v+B)\right]=\mathcal{H}\frac{\bar{\rho}}{\bar{\rho}'}\Delta \tag{2.109}$$

that so is proportional to the comoving-gauge density contrast (2.92). Besides, the Fourier transformation has been applied on (2.91),

$$-k^2\Phi_{\mathbf{k}}=\frac{3}{2}\mathcal{H}^2\Delta_{\mathbf{k}}. \tag{2.110}$$

$$\Rightarrow\quad \Delta_{\mathbf{k}}=-\frac{2}{3}\left(\frac{k}{\mathcal{H}}\right)^2\Phi_{\mathbf{k}}. \tag{2.111}$$

On $k\ll 1$ super-horizon scales, $\Delta_{\mathbf{k}}\approx 0$. Hence,

$$\mathcal{R}_{\mathbf{k}}\approx\zeta_{\mathbf{k}},\qquad \text{in super-horizon scales.} \tag{2.112}$$

Furthermore, it can be proved that ζ is conserved on super-horizon. Another useful property of this arises when writing (2.96) in Fourier space as well, it hence can be expressed as,

$$-k^2\Phi_{\mathbf{k}}-3\mathcal{H}(\Phi'+\mathcal{H}\Phi)=\frac{3}{2}\mathcal{H}^2\delta_{\mathbf{k}}. \tag{2.113}$$

Then, isolating $\delta_{\mathbf{k}}$,

$$\delta_{\mathbf{k}}=-\frac{2}{3}\left(\frac{k^2}{\mathcal{H}^2}+3\right)\Phi-2\left(\frac{\Phi'}{\mathcal{H}}\right). \tag{2.114}$$

In terms of Newtonian gauge variables, the quantity defined in (2.108) is,

$$\begin{aligned}\mathcal{R}_{\mathbf{k}}=\Phi_{\mathbf{k}}-\mathcal{H}v=&\ \Phi_{\mathbf{k}}+\mathcal{H}\left(\frac{\Phi'_{\mathbf{k}}+\mathcal{H}\Phi_{\mathbf{k}}}{4\pi G a^2(\bar{\rho}+\bar{P})}\right)\\ =&\ \Phi_{\mathbf{k}}+\frac{2}{3}\left(\frac{\mathcal{H}^{-1}\Phi'_{\mathbf{k}}+\Phi_{\mathbf{k}}}{1+\frac{\bar{P}}{\bar{\rho}}}\right).\end{aligned} \tag{2.115}$$

As we saw on the previous dark matter case. $\Phi_{\mathbf{k}}=\Psi_{\mathbf{k}}=const.$ on super-horizon scales. Thus, $\mathcal{R}_{\mathbf{k}}\approx\frac{5}{3}\Phi_{\mathbf{k}}$. Relating (2.114) and (2.115), one may express $\delta_{\mathbf{k}}$ as a function of $\mathcal{R}_{\mathbf{k}}$ as follows,

$$\delta_{\mathbf{k}}=-\frac{2}{5}\left(\frac{k^2}{\mathcal{H}^2}+3\right)\mathcal{R}_{\mathbf{k}}. \tag{2.116}$$

This result is extremely important because relates the perturbations with matter perturbations.

2.7 ADM-FLRW coordinates

In order to make contact with the quantities employed by numerical simulations of gravitational collapse (see [Torres et al., 2014]), the perturbative FLRW metric in Newtonian gauge in spherical coordinates. In this section was following from Nuñez et al. Private communication.

$$ds^2 = -(1+2\Phi)dT^2 + a(T)^2(1-2\Psi)(dR^2 + R^2 d\Omega^2). \tag{2.117}$$

For a perfect fluid or scalar field, there are no anisotropic stresses and the field equations $i = j$ ensures $\Phi = \Psi$. The product $a(T)^2(1-2\Psi)$ is changed by $\exp(2\psi)$, where $\psi = \psi(R,T)$, so that the line element takes the next form,

$$ds^2 = -(1+2\Phi)dT^2 + \exp(2\psi)(dR^2 + R^2 d\Omega^2). \tag{2.118}$$

Using the coordinates transformation,

$$T \to t, \qquad \text{and} \qquad R \to r\exp(-\psi), \tag{2.119}$$

$$\begin{aligned} \Rightarrow \quad dT = dt, \quad \text{and} \quad dR &= \exp(-\psi)(dr - rd\psi) \\ &= \exp(-\psi)(dr - r\dot{\psi}dt - r\psi' dr). \end{aligned} \tag{2.120}$$

The line element then is rewritten as,

$$ds^2 = -(1+2\Phi)dt^2 + r^2 d\Omega^2 + (1-r\psi')^2\left(dr - \frac{r\dot{\psi}}{(1-r\psi')}dt\right)^2. \tag{2.121}$$

Defining the functions,

$$\alpha^2 = 1 + 2\Phi. \tag{2.122}$$

$$\gamma = 1 - r\psi'. \tag{2.123}$$

$$\beta = -\frac{r\dot{\psi}}{\gamma}. \tag{2.124}$$

The line element takes the form of an ADM-like (Arnowitt-Deser-Misner) one where we have defined the radial coordinate, r as the areal radius.

$$ds^2 = -\alpha^2 dt^2 + \gamma^2\left(dr + \beta dt\right)^2 + r^2 d\Omega^2, \tag{2.125}$$

with α and β the lapse and shift functions, and γ the $r-r$ component in the constant time hypersurface. At this point we could continue and obtain the corresponding form of the Einstein equations in such coordinate system. However, for this case was convenient go a step further and define the following functions,

$$\nu = \frac{\beta}{\alpha}. \tag{2.126}$$

$$m = \frac{r}{2}\left(1 + \nu^2 - \gamma^{-2}\right). \tag{2.127}$$

$$\Delta = 1 - 2\frac{m}{r} + \nu^2 = \gamma^{-2}. \tag{2.128}$$

Expanding the terms of (2.125),

$$ds^2 = -\left(\alpha^2 - \gamma^2\beta^2\right)dt^2 + \gamma^2 dr^2 + 2\gamma^2\beta dr dt + r^2 d\Omega^2. \tag{2.129}$$

Also using the expressions (2.126), (2.127) and (2.128).

$$ds^2 = -\frac{\alpha^2}{\Delta}\left(\Delta - \nu^2\right)dt^2 + 2\,\frac{\alpha\,\nu}{\Delta}dr dt + \frac{dr^2}{\Delta} + r^2 d\Omega^2. \tag{2.130}$$

Finally we have obtained the ADM-FLRW metric,

$$ds^2 = -\frac{\alpha^2}{\Delta}\left(1 - 2\frac{m}{r}\right)dt^2 + 2\,\frac{\alpha\,\nu}{\Delta}dr dt + \frac{dr^2}{\Delta} + r^2 d\Omega^2. \tag{2.131}$$

Notice that temporal component has a term almost similar to that of the Schwarzschild metric. This form of the line element implies a very simple expression for the mixed Einstein tensor components obtained as,

$$G^t_t = -2\,\frac{m'}{r^2}. \tag{2.132}$$

$$G^r_t = 2\,\frac{\dot{m}}{r^2}. \tag{2.133}$$

$$G^t_r = \frac{2\,r^2\nu\,\dot{\nu} - 2\,r\,\dot{m} - 2\,\alpha\,m\,\nu}{r^3\alpha^2\,\Delta}. \tag{2.134}$$

$$G^r_r = \frac{2r^3\,\dot{\nu} + 2r^2\,\nu\,\dot{m} - 4r^2\,m\,\dot{\nu} - 2r\,\alpha\,m + 4\alpha\,m^2}{r^4\alpha\,\Delta}. \tag{2.135}$$

The final remark about this formalism: Those coordinates are certainly more applicable in Numerical Relativity (that is the reason they are called ADM-FLRW coordinates), but we can briefly discuss their particularities. On one hand, the advantages being that Einstein differential equations are transforming from 2nd order into 1st order. On the other hand, we have to be careful because there are too many functions to determine and it is necessary to find the constraints and extra relations between each other.

Chapter 3

Homogeneous scalar field during Reheating

«Everything we call real is made of things that cannot be regarded as real»
Niels Bohr

Since we have derived all expressions that just will need through this chapter. At large scales according to cosmological principle the background is homogeneous and isotropic, which is the pure FLRW case, mathematically all the background quantities[1] cannot depend on the spatial coordinates. Also that forces us setting up $\Phi = \Psi = 0$ from the Eq. (2.117). By now our first step is to obtain the metric components.

$$\psi_0 = \psi_0(t) = \ln(a), \quad \Rightarrow \quad H = \dot{\psi_0}. \tag{3.1}$$

Actually it is easy to compute the functions (2.122), (2.123), (2.124), (2.126), (2.127) and (2.128) for this case.

$$\alpha_0 = 1, \tag{3.2}$$

$$\gamma_0 = 1, \tag{3.3}$$

$$\beta_0 = -rH, \tag{3.4}$$

$$\nu_0 = -rH, \tag{3.5}$$

$$m_0 = \frac{1}{2} r^3 H^2, \tag{3.6}$$

$$\Delta_0 = 1. \tag{3.7}$$

Reheating arose after the inflationary epoch when the scalar field goes down to the effective potential minimum. Although, when the scalar field oscillated over minimum potential could be modeled by different ways as we shown in Figure 1.7, we choose an harmonic potential $V = \mu^2|\phi|^2$ for technical simplicity and since formally this represents the first term in a Taylor expansion near a potential minimum. We also did not consider self-interactions for the meantime. The energy-momentum tensor is thus,

$$T_{\mu\nu} = \partial_\mu \phi^* \partial_\nu \phi + \partial_\mu \phi \partial_\nu \phi^* - g_{\mu\nu} \left(\partial^\alpha \phi \partial_\alpha \phi^* + \mu^2 \phi \phi^* \right). \tag{3.8}$$

with $\mu = \frac{mc}{\hbar}$ being the scalar field mass on natural units. As long as isotropy and homogeneity is preserved, the scalar field only depends of time $\phi(t, \vec{r}) = \phi_0(t)$. By now we might be able to compute the density of scalar field through

[1] Hereinafter the sub index 0 will represent background quantities.

the expression (1.25) but first we need the normal vector n^μ to the t =const. surfaces which has the explicit components,

$$n^\mu = (1, r\,H(t), 0, 0). \tag{3.9}$$

Then, the non-zero terms of energy density (1.25) are,

$$\rho_0 = n^0 n^0 T_{00} + n^0 n^1 T_{01} + n^1 n^0 T_{10} + n^1 n^1 T_{11}. \tag{3.10}$$

$$\rho_0 = \Pi_0\,\Pi_0^* + \mu^2 \phi_0\,\phi_0^*, \tag{3.11}$$

and the pressure is given by the expression (1.26),

$$P_0 = \Pi_0\,\Pi_0^* - \mu^2 \phi_0\,\phi_0^*, \tag{3.12}$$

where we have defined the momentum $\Pi_0 \equiv \dot{\phi_0}$.
Indeed these above expressions represent constraint equations. Clearly we need a evolution equation which has been obtained by (1.10),

$$\dot{\Pi}_0 + 3H\Pi_0 + \mu^2\phi_0 = 0. \tag{3.13}$$

It determines the time evolution of the H and the scalar field ϕ_0. Then,

$$H^2 = \frac{8\pi G}{3}\left(\Pi_0\Pi_0^* + \mu^2\phi_0\phi_0^*\right). \tag{3.14}$$

Friedmann equation (1.43) has been used to close the system equations.

3.1 Analytic solution approximations to Reheating

At this point we would wish solve Eq. (3.13), unfortunately it does not have an analytic solution. However, in this case we will concentrate oscillations around near the minimum as is shown in Figure 1.6. During Reheating the expansion rate of the Universe is slower compared to time of oscillation of the scalar field. In other words the scalar field oscillation is faster than Hubble expansion, $t_H = (aH)^{-1} \gg (a\mu)^{-1} = t_\phi$, or $H \ll \mu$. This inequality is always satisfied at late times, and it is helpful to find an approximated solutions.

One important condition from the end of the inflationary epoch is $\epsilon = 1$. In view of (3.12),

$$P_0 = 0 \quad \rightarrow \quad \Pi_0\,\Pi_0^* = \mu^2\phi_0\,\phi_0^*. \tag{3.15}$$

The scalar field has a behavior as pressure-less “fluid", even though, in reality it cannot be exactly dust with $P = 0$ but it behaves either as a “fluid" with small pressure or as a collisionless “fluid". The density (3.11) provides the next relation,

$$\rho_0 = 2\mu^2|\phi_0|^2. \tag{3.16}$$

Since this scenario is approaching as pressure-less background, we thus already know how the background density scales at matter epoch (1.51). Therefore we had proposed the following Ansatz as,

$$\phi_0 \sim a^{-\frac{3}{2}}. \tag{3.17}$$

And we futher propose a general solution as,

$$\phi_0 = f(t)\, a^{-\frac{3}{2}}. \tag{3.18}$$

This give us a differential equation for $f(t)$,

$$\mu^2 f + \ddot{f} - \frac{3af\,\ddot{a}}{2\,a^2} - \frac{3f\,\dot{a}^2}{4\,a^2} = 0. \tag{3.19}$$

Besides, due to $\mu \gg H$ the Eq. (3.19) would be simplified to,

$$\ddot{f} + \mu^2 f = 0. \tag{3.20}$$

This assumption drive us towards an harmonic oscillator equation! This has the famous flat waves solution,

$$f(t) = C_1 \exp(i\mu t) + C_2 \exp(-i\mu t). \tag{3.21}$$

Therefore to simplify the above solution, we have set another form of the solution with a constant phase ψ_0,

$$\phi_0(t) = C\, a^{-\frac{3}{2}} \exp(i(\mu t + \psi_0)). \tag{3.22}$$

In the simplified case of a real scalar field,

$$\phi_0(t) = A\, a^{-\frac{3}{2}} \sin(\mu t + \theta_0). \tag{3.23}$$

With A and C being integration constants. The background real case has been followed in [Alcubierre et al., 2015] and it will be discussed on Appendix A. The background complex case in cosmological context is discussed in [Jetzer and Scialom, 1997].

3.2 Initial conditions

Since initially the scalar field is described like a pressure-less “fluid", the background would have had at the initial time, specifically the end of inflation t_{end}, the values $H(t_{end}) = H_{end}$, $a(t_{end}) = a_{end}$ and $P(t_{end}) = P_{end} = 0$,

$$H^2_{end} = \frac{1}{3M^2_{Pl}} \left(|\Pi|^2_{end} + \mu^2 |\phi|^2_{end} \right). \tag{3.24}$$

Here we have used the reduced Planck mass $M^2_{Pl} \equiv \dfrac{1}{8\pi G}$, thus,

$$P_{end} = |\Pi|^2_{end} - \mu^2 |\phi|^2_{end}. \tag{3.25}$$

The scale factor in pressure-less or dust scenario goes like shown in Table 1.1 and making use of analytic solution (3.22) and its derivative, with conditions (3.24) and (3.25) one would calculate the integration constant as follows,

$$C = \left(\frac{\sqrt{H^2_{end} - \kappa P_{end}}}{\sqrt{2\kappa}\mu} \right) a^{\frac{3}{2}}_{end} \exp(-i(\mu t_{end} + \psi_0)) \tag{3.26}$$

Hence,

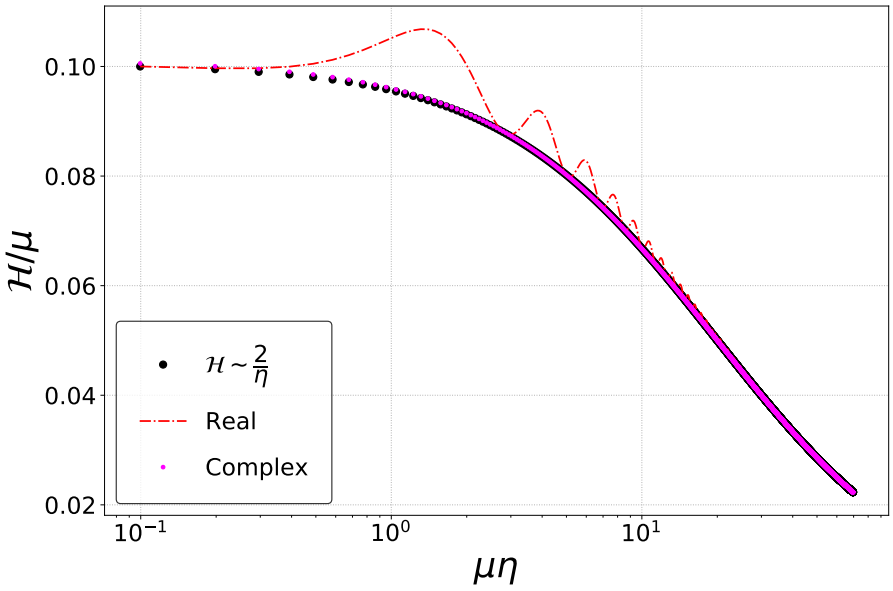

Figure 3.1: Evolution of the conformal Hubble parameter $\mathcal{H}/\mu$ as a function of $\mu\eta$ with a value of $\mu = 10H_{end}$ for a real/complex scalar field oscillating around the minimum of the potential. We show the comparison between the solution of standard dust with **black** dots, and both analytical approximations (3.23) in red line-dots and (3.22) in magenta tiny dots.

$$\phi_0(t) = \left(\frac{\sqrt{H_{end}^2 - \kappa P_{end}}}{\sqrt{2\kappa}\mu}\right)\left(\frac{t_{end}}{t}\exp[i\mu(t-t_{end})]\right). \tag{3.27}$$

Then, evaluated at t_{end},

$$\phi_{end} = \frac{\sqrt{H_{end}^2 - \kappa P_{end}}}{\sqrt{2\kappa}\mu}. \tag{3.28}$$

Interestingly the phase ψ_0 does not appear on the initial condition. We also derived (3.27) to find an expression for the momentum,

$$\Pi_0(t) = i\mu\phi_0(t) - \frac{3}{2}H\phi_0(t). \tag{3.29}$$

Evaluated at t_{end}, we will find the second initial condition,

$$\Pi_{end} = i\mu\phi_{end} - \frac{3}{2}H_{end}\,\phi_{end}. \tag{3.30}$$

As an example relating the scalar field ϕ to inflaton, one could set the initial value of H_{end} at the end of inflation based on [Martin et al., 2019] being $\rho_{inf} = 3H_{end}^2$ $\mathrm{M}_{Pl}^2 = 10^{12}$ $\mathrm{M}_{Pl}^4 = 2.43 \times 10^{15}$ GeV so that corresponds to $H_{end} \sim 10^{-6}$ M_{Pl}. Even though, the condition $H \ll \mu$ is not met at the end of inflation see Figure 3.2. The approximation (3.22) rapidly converges towards the numerical solution generated with the same conditions, despite the oscillations are still evident, but

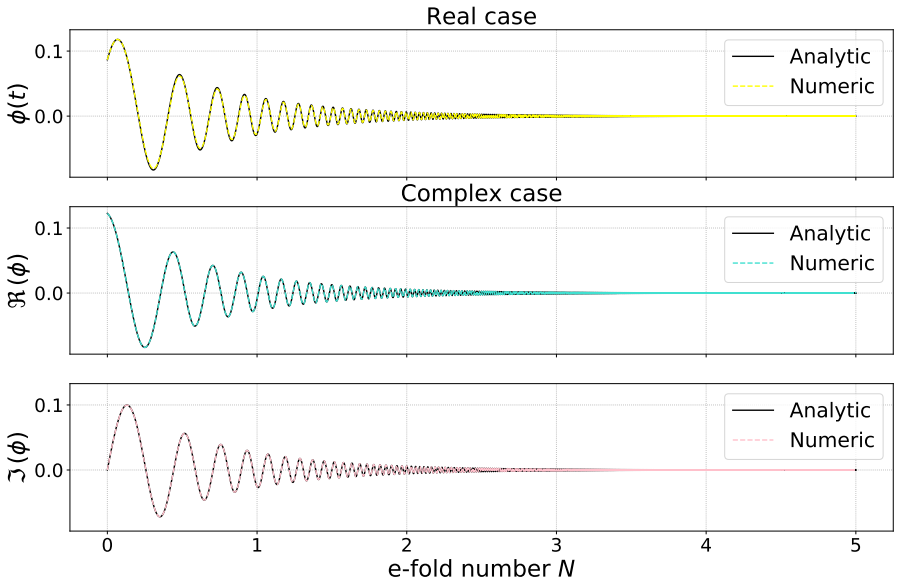

Figure 3.2: The background solution is numerically compared to analytical for both cases have a value of $n = 10$.

their amplitude decreases as time goes by. If we assume that $\mu = nH_{end}$ then, the initial condition (3.28) would be rewritten as,

$$\phi_{end} = \sqrt{\frac{3}{2}}\frac{1}{n}\,\mathrm{M}_{Pl}. \tag{3.31}$$

The above equation, on the fast oscillations regime must meet the condition $n >> 1$. Thus, it certainly is translated to find $\phi_{end} \ll \mathrm{M}_{Pl}$. In light of the definition of the slow roll parameter (1.71), the last condition implies that the Universe is out of the period of slow-roll. Note finally that in Figure 3.3 the complex solution shows no oscillations for the Hubble parameter as well as for the pressure. As seen in the Figure 3.1, this characteristic is not shared with the real field.

In the next chapter we will analyze the behavior of small perturbations around the homogeneous solution (3.27). Furthermore, we would like to determine the instability band located between Hubble horizon and Jeans length which will provide us several scales where the perturbations might grow.

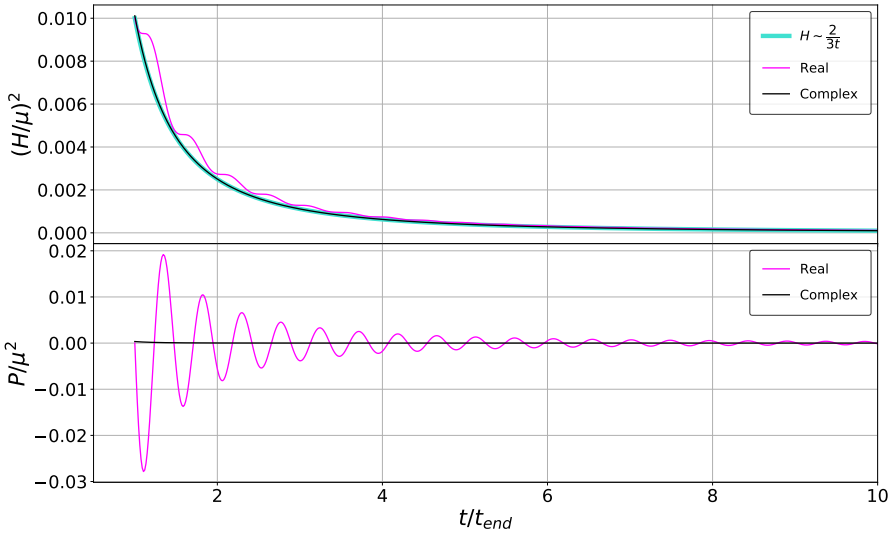

Figure 3.3: The first plot shows how the constraint Eq. (3.14) evolves for both the real and complex scalar field compared to the solution in standard pressure-less dust. The second plot shows that an oscillatory solution behaves in average like a pressure-less “fluid" for the real case. Otherwise the complex case behaves completely as pressure-less. Here we have used a value $\mu = 10H_{end}$.

Chapter 4

Evolution of perturbations during Reheating

«As usual, nature's imagination far surpasses our own. As we have seen from the other theories, they are really quite subtle and deep»

Richard Feynman

The aim of this chapter is to describe how the tiny fluctuations or perturbations during Reheating evolved. Furthermore we focus on a complex scalar field without a quartic self-interaction in a perturbed FLRW Universe and only perturbations at linear order will be considered. For that reason, the scalar field is expressed as,

$$\phi = \phi_0(t) + \phi_1(x^i, t). \tag{4.1}$$

Where $\frac{\phi_1}{\phi_0} \ll 1$. For our purposes it is convenient to start with the perturbed comoving FLRW metric (1.58), in Newtonian gauge and comparable to ADM so that the results will be transferable to initial collapse conditions of Section 2.7.

$$ds^2 = a(\eta)^2[-(1+2\Phi)d\eta^2 + (1-2\Psi)(dR^2 + R^2 d\Omega^2)]. \tag{4.2}$$

Note that we are using the conformal time instead of cosmic time to express the metric. In term of this variable, the relevant Einstein field equations are[1],

$$^{(0)}G^{\eta}_{\eta} \qquad \rightarrow \qquad \mathcal{H}^2 = \frac{8\pi G}{3} a^2 \rho_0. \tag{4.3}$$

$$^{(0)}G^{r}_{r} \qquad \rightarrow \qquad \mathcal{H}' - \mathcal{H}^2 = -4\pi G a^2(\rho_0 + P_0). \tag{4.4}$$

The background density (1.25) is,

$$\rho_0 = \frac{\phi_0' \phi_0'^*}{a^2} + \mu^2 \phi_0 \phi_0^*, \tag{4.5}$$

and the pressure given by (1.26) is

$$P_0 = \frac{\phi_0' \phi_0'^*}{a^2} - \mu^2 \phi_0 \phi_0^*. \tag{4.6}$$

As a result of the conservation law (1.10) is the Klein-Gordon equation,

$$\phi_0'' + 2\mathcal{H}\phi_0' + a^2\mu^2\phi_0 = 0. \tag{4.7}$$

As mentioned before, these are purely background quantities. These conformal background expressions are going to be useful in order to obtain the perturbed equations.

[1] The superscript $^{(n)}G$ denotes the n-th order in perturbative expansion.

Including the perturbed scalar field (4.1) on Einstein equations (1.2) at linear order, the components ${}^{(1)}G^{\eta}_{\eta}$ and ${}^{(1)}G^{r}_{\eta}$ field equations respectively are,

$$\begin{aligned}\Delta\Psi - 3\mathcal{H}(\Psi' + \mathcal{H}\Phi) =& 4\pi G(a^2\mu^2\phi_0^*\phi_1 + a^2\mu^2\phi_0\phi_1^* \\ &+ \phi_0'^*\phi_1' + \phi_0'\phi_1'^* - 2\phi_0'\phi_0'^*\Phi). \end{aligned} \tag{4.8}$$

$$\Psi' + \mathcal{H}\Phi = 4\pi G(\phi_0'\phi_1^* + \phi_0'^*\phi_1). \tag{4.9}$$

Additionally due to azimuthal symmetry ${}^{(1)}G^{\theta}_{\theta}$ and ${}^{(1)}G^{\varphi}_{\varphi}$ are the same. From this we can show that there is no anisotropic stress tensor Π_{ij} at 1st order. The proof comes from taking the differences between,

$$G^r_r - G^\theta_\theta = 8\pi G(\,T^r_r - \,T^\theta_\theta\,). \tag{4.10}$$

This guarantees that,

$$\frac{d^2\,(\Psi-\Phi)}{dR^2} - \frac{1}{R}\frac{d\,(\Psi-\Phi)}{dR} = \left(\frac{28\pi G}{1-2\Phi}\right)\frac{d\phi_1}{dR}\frac{d\phi_1^*}{dR}. \tag{4.11}$$

The right hand side is a second order term, so we can safely neglected it at linear order and this implies,

$$\Phi = \Psi. \iff \Pi_{ij} = 0. \tag{4.12}$$

Thus, the Eq. (4.8) can be cast as,

$$\begin{aligned}\Delta\left(\frac{a^2\Psi}{\mathcal{H}}\right) = \frac{4\pi G a^2}{\mathcal{H}}&\left(a^2\mu^2\phi_0^*\phi_1 + a^2\mu^2\phi_0\phi_1^* + \phi_0'^*\phi_1' + \phi_0'\phi_1'^*\right. \\ &\left.-2\phi_0'\phi_0'^*\Psi\right) + 3a^2(\Psi' + \mathcal{H}\Psi). \end{aligned} \tag{4.13}$$

From now on, the background equations will be useful in order to reduce our perturbative equations. For instance, we can substitute (4.3) in the above equation and find that,

$$\begin{aligned}\Delta\left(\frac{a^2\Psi}{\mathcal{H}}\right) = &\frac{4\pi G a^2}{\mathcal{H}}\left(a^2\mu^2\phi_0^*\phi_1 + a^2\mu^2\phi_0\phi_1^* + \phi_0'^*\phi_1' + \phi_0'\phi_1'^*\right) \\ &+ 3a^2\Psi' + \frac{8\pi G a^4\mu^2}{\mathcal{H}}\phi_0\phi_0^*\Psi. \end{aligned} \tag{4.14}$$

The next highlighted blue terms represent numerically a factor of one derived from the background Eq. (4.3),

$$\begin{aligned}\Delta\left(\frac{a^2\Psi}{\mathcal{H}}\right) = &\frac{4\pi G a^2}{\mathcal{H}}\left(a^2\mu^2\phi_0^*\phi_1 + a^2\mu^2\phi_0\phi_1^* + \phi_0'^*\phi_1' + \phi_0'\phi_1'^*\right) \\ &+ \frac{8\pi G a^4\mu^2}{\mathcal{H}}\phi_0\phi_0^*\Psi + 3a^2\Psi'\left[\frac{8\pi G\left(\phi_0'\phi_0'^* + a^2\mu^2\phi_0\phi_0^*\right)}{3\mathcal{H}^2}\right]. \end{aligned} \tag{4.15}$$

Then,

$$\begin{aligned}\Delta\left(\frac{a^2\Psi}{\mathcal{H}}\right) = 4\pi G&\left[\frac{a^4\mu^2}{\mathcal{H}}\left(\phi_0^*\phi_1 + \phi_0\phi_1^*\right) + \frac{a^2}{\mathcal{H}}\left(\phi_0'^*\phi_1' + \phi_0'\phi_1'^*\right)\right. \\ &\left.+\frac{2a^2\phi_0'\phi_0'^*\Psi'}{\mathcal{H}^2}\right] + \frac{8\pi G a^4\mu^2}{\mathcal{H}^2}\phi_0\phi_0^*\Psi' + \frac{8\pi G a^4\mu^2}{\mathcal{H}}\phi_0\phi_0^*\Psi. \end{aligned} \tag{4.16}$$

In the last two terms outside of square parenthesis, we identify our Eq. (4.9),

$$\Delta\left(\frac{a^2\Psi}{\mathcal{H}}\right) = 4\pi G\left[\frac{a^4\mu^2}{\mathcal{H}}\left(\phi_0^*\phi_1+\phi_0\phi_1^*\right)+\frac{a^2}{\mathcal{H}}\left(\phi_0'^*\phi_1'+\phi_0'\phi_1'^*\right)\right.$$
$$+2a^2\phi_0'\phi_1^* - 2a^2\phi_0'\phi_1^* +2a^2\phi_0'^*\phi_1 - 2a^2\phi_0'^*\phi_1$$
$$\left.+\frac{2a^2\phi_0'\phi_0'^*\Psi'}{\mathcal{H}^2}\right]+\frac{8\pi G a^4\mu^2}{\mathcal{H}^2}\phi_0\phi_0^*\left[4\pi G(\phi_0'\phi_1^*+\phi_0'^*\phi_1)\right]. \tag{4.17}$$

We can complete the Klein-Gordon equation (4.7), so factorising and accommodating,

$$\Delta\left(\frac{a^2\Psi}{\mathcal{H}}\right) = 4\pi G\left[\frac{a^2\phi_0'\phi_1'^*}{\mathcal{H}}+\frac{a^2\phi_0'^*\phi_1'}{\mathcal{H}}+\frac{2a^2\phi_0'\phi_0'^*\Psi'}{\mathcal{H}^2}\right.$$
$$+\frac{8\pi G a^4\mu^2}{\mathcal{H}^2}\phi_0\phi_0^*\left[\cancel{\phi_0'\phi_1^*}+\cancel{\phi_0'^*\phi_1}\right]-\frac{a^2\phi_1^*}{\mathcal{H}}\left(-2\mathcal{H}\phi_0'-a^2\mu^2\phi_0\right)$$
$$+a^2\phi_0'\phi_1^*\left[1-\frac{8\pi G\left(\phi_0'\phi_0'^*+\cancel{a^2\mu^2\phi_0\phi_0^*}\right)}{\mathcal{H}^2}\right]-\frac{a^2\phi_1}{\mathcal{H}}\left(-2\mathcal{H}\phi_0'^*\right.$$
$$\left.\left.-a^2\mu^2\phi_0^*\right)+a^2\phi_0'^*\phi_1\left[1-\frac{8\pi G\left(\phi_0'\phi_0'^*+\cancel{a^2\mu^2\phi_0\phi_0^*}\right)}{\mathcal{H}^2}\right]\right]. \tag{4.18}$$

Actually we have rewritten the acceleration equation (4.4) as,

$$\frac{\mathcal{H}'}{\mathcal{H}^2}-1=-\frac{8\pi G}{\mathcal{H}^2}\phi_0'\phi_0'^*. \tag{4.19}$$

Then rearranging,

$$\Delta\left(\frac{a^2\Psi}{\mathcal{H}}\right) = 4\pi G\left[\frac{a^2\phi_0'\phi_1'^*}{\mathcal{H}}+\frac{a^2\phi_0'\phi_0'^*\Psi'}{\mathcal{H}^2}-\frac{a^2\phi_1^*\phi_0''}{\mathcal{H}}+a^2\phi_0'\phi_1^*\frac{\mathcal{H}'}{\mathcal{H}}\right.$$
$$+\frac{a'a\phi_0'\phi_1^*}{\mathcal{H}}-\frac{a'a\phi_0'\phi_1^*}{\mathcal{H}}+\frac{a^2\phi_0'^*\phi_1'}{\mathcal{H}}+\frac{a^2\phi_0'\phi_0'^*\Psi'}{\mathcal{H}^2}$$
$$\left.-\frac{a^2\phi_1\phi_0''^*}{\mathcal{H}}+a^2\phi_0'^*\phi_1\frac{\mathcal{H}'}{\mathcal{H}}+\frac{a'a\phi_0'^*\phi_1}{\mathcal{H}}-\frac{a'a\phi_0'^*\phi_1}{\mathcal{H}}\right]. \tag{4.20}$$

The above equation simplifies enormously when written in terms of the Mukhanov-Sasaki (M-S) variable. This is defined as,

$$u\equiv a\phi_1+z\Psi, \qquad \text{where} \qquad z\equiv\frac{a\phi_0'}{\mathcal{H}}. \tag{4.21}$$

The Eq. (4.18) then takes the form,

$$\Delta\left(\frac{a^2\Psi}{\mathcal{H}}\right) = 4\pi G\left[a'z\phi_1^*+az\phi_1'^*+z\Psi'z^*-a\phi_1^*z'+z\Psi z'^*-z\Psi z'^*\right.$$
$$\left.+a'z^*\phi_1+az^*\phi_1'+z\Psi'z^*-a\phi_1z'^*+z^*\Psi z'-z^*\Psi z'\right]. \tag{4.22}$$

From this final form, we can reduce the equation considerably by employing the M-S variable, this may be expressed as,

$$\Delta\left(\frac{a^2\Psi}{\mathcal{H}}\right) = 4\pi G\left(u'^*z - u^*z' + u'z^* - uz'^*\right). \tag{4.23}$$

This first result is one of two elements necessary in order to find the evolution equation for the M-S variable. Proceeding in the same fashion with Eq. (4.9),

$$\frac{a^2\Psi'}{\mathcal{H}} + a^2\Psi = \frac{4\pi G a^2}{\mathcal{H}}(\phi_0'\phi_1^* + \phi_0'^*\phi_1). \tag{4.24}$$

$$\frac{a^2\Psi'}{\mathcal{H}} + 2a^2\Psi - a^2\Psi + \frac{8\pi G a^2}{\mathcal{H}^2}\phi_0'\phi_0'^*\Psi = + \frac{4\pi G a^2}{\mathcal{H}}(\phi_0'\phi_1^* + \phi_0'^*\phi_1) + \frac{8\pi G a^2}{\mathcal{H}^2}\phi_0'\phi_0'^*\Psi. \tag{4.25}$$

Now we can use the expression (4.19) into (4.25),

$$\frac{a^2\Psi'}{\mathcal{H}} + 2a^2\Psi - \frac{a^2\mathcal{H}'}{\mathcal{H}^2}\Psi = \frac{4\pi G a^2}{\mathcal{H}}\left(\phi_0'\phi_1^* + \phi_0'^*\phi_1 + \frac{2\phi_0'\phi_0'^*\Psi}{\mathcal{H}}\right). \tag{4.26}$$

Again making use of the M-S variable (4.21),

$$\left(\frac{a^2\Psi}{\mathcal{H}}\right)' = 4\pi G\left(az\phi_1^* + az^*\phi_1 + 2zz^*\Psi\right), \tag{4.27}$$

which implies,

$$\left(\frac{a^2\Psi}{\mathcal{H}}\right)' = 4\pi G\left(u^*z + uz^*\right). \tag{4.28}$$

This formulation is particularly convenient to relate the conformal time derivative of (4.23) and the Laplacian of (4.28),

$$\left(u'^*z - u^*z'\right)' + \left(u'z^* - uz'^*\right)' - \Delta\left(u^*z + uz^*\right) = 0. \tag{4.29}$$

Reducing,

$$u''^*z - u^*z'' + u''z^* - uz''^* - z\Delta u^* - z^*\Delta u = 0, \tag{4.30}$$

and accommodating terms,

$$\left[u''^* - \Delta u^* - \frac{z''}{z}u^*\right]z + \left[u'' - \Delta u - \frac{z''^*}{z^*}u\right]z^* = 0. \tag{4.31}$$

So that above equation to be fulfilled, the following must be satisfied that,

$$u''^* - \Delta u^* - \frac{z''}{z}u^* = 0, \qquad \text{and} \qquad u'' - \Delta u - \frac{z''^*}{z^*}u = 0. \tag{4.32}$$

Even though, in the complex case the equations are a bit more complicated than the real case, their structure is similar.
The evolution of real scalar field fluctuations during Reheating has been studied by several authors (see for example [Jedamzik et al., 2010], [Alcubierre et al., 2015], [Hidalgo et al., 2017] and [Martin et al., 2019]).

A common strategy to solve (4.32) is to write them in Fourier space. Then $u_{\mathbf{k}}$ evolves according to,

$$u''^{*}_{\mathbf{k}} + \left(k^2 - \frac{z''}{z}\right) u^{*}_{\mathbf{k}} = 0 \qquad \text{and} \qquad u''_{\mathbf{k}} + \left(k^2 - \frac{z''^{*}}{z^{*}}\right) u_{\mathbf{k}} = 0 \tag{4.33}$$

Every $k-$mode represents a scale. Note that each equation is the conjugate of the other. First of all, in order to solve these equations it is necessary to compute the expression $\frac{z''}{z}$. Fortunately the function $z(\eta)$ depends only on the background quantities,

$$\frac{z''}{z} = 2\left(\frac{\mathcal{H}'}{\mathcal{H}}\right)^2 - \frac{\mathcal{H}''}{\mathcal{H}} - 2\mathcal{H}' + \frac{a''}{a} - \frac{2\mathcal{H}'\phi_0''}{\mathcal{H}\phi_0'} + \frac{2\mathcal{H}\phi_0''}{\phi_0'} + \frac{\phi_0'''}{\phi_0'}. \tag{4.34}$$

Since the background complex scalar field presents no pressure at all, the above equation can be simplified by making use of the following background equations.

$$\frac{\mathcal{H}'}{\mathcal{H}^2} - 1 = -\frac{4\pi G a^2 \rho_0}{\mathcal{H}^2}, \quad \Rightarrow \quad \mathcal{H}' = -\frac{1}{2}\mathcal{H}^2, \tag{4.35}$$

$$\text{and} \quad \mathcal{H}'' = -\mathcal{H}\mathcal{H}' = \frac{1}{2}\mathcal{H}^3. \tag{4.36}$$

Then,

$$\frac{a''}{a} = \mathcal{H}' + \mathcal{H}^2 = \frac{1}{2}\mathcal{H}^2. \tag{4.37}$$

If we substitute the above quantities and the Klein-Gordon equation (4.7) in the expression (4.34), we find

$$\begin{aligned}\frac{z''}{z} = {} & 2\left(\frac{1}{4}\mathcal{H}^2\right) - \frac{1}{2}\mathcal{H}^2 + \mathcal{H}^2 + \frac{1}{2}\mathcal{H}^2 + \frac{3\mathcal{H}}{\phi_0'}\left(-2\mathcal{H}\phi_0' - \mu^2 a^2 \phi_0\right) \\ & + \frac{1}{\phi_0'}\left(-2\mathcal{H}'\phi_0' - 2\mathcal{H}\phi_0'' - \mu^2 a^2 \phi_0' - 2\mu^2 a a' \phi_0\right).\end{aligned} \tag{4.38}$$

Reducing terms,

$$\begin{aligned}\frac{z''}{z} = {} & -\frac{9}{2}\mathcal{H}^2 - \frac{3\mathcal{H}\mu^2 a^2 \phi_0}{\phi_0'} + \frac{1}{\phi_0'}\left[\mathcal{H}^2\phi_0' - 2\mathcal{H}\left(-2\mathcal{H}\phi_0' - \mu^2 a^2 \phi_0\right)\right. \\ & \left. -\mu^2 a^2 \phi_0' - 2\mu^2 a a' \phi_0\right],\end{aligned} \tag{4.39}$$

and,

$$\frac{z''}{z} = -\mu^2 a^2 + \frac{1}{2}\mathcal{H}^2 - \frac{3\mathcal{H}\mu^2 a^2 \phi_0}{\phi_0'}. \tag{4.40}$$

The scale $|z''/z|^{\frac{1}{2}}$ determines the Jeans wavenumber or Jeans Scale k_J. It is important to remark that this expression is not equivalent to that in the M-S equation in the real case. This is looked at in detail in Appendix A.
Since the background solution is approximated by $\phi_0 \sim a^{-\frac{3}{2}} \exp[i(\mu t + \psi_0)]$, we may express (4.40) in analytic (approximate) form as follows,

$$\frac{z''}{z} = \frac{1}{2}\mathcal{H}^2 - \mu^2 a^2 \left[1 + \frac{3\mathcal{H}}{\left(ia\mu - \frac{3}{2}\mathcal{H}\right)}\right]. \tag{4.41}$$

As long as we are in an oscillatory regime $\mu \gg H$, the Eq. (4.41) can be further reduced to,

$$\frac{z''}{z} = -\mu^2 a^2 + i\,3\mu a\mathcal{H}. \tag{4.42}$$

In order to analyze this perturbed complex scalar field, we solve equations (4.33) numerically since they do not have the complete analytic solutions. In this chapter we obtain approximate analytic solutions by regimes divided by the Jeans scale.
The first regime is when the $k-$modes are considerably larger in size than the Jeans scale, i.e. $k^2 \ll z''/z$. The other extreme, when they are much smaller than the Jeans scale, i.e. $k^2 \gg z''/z$ is the oscillatory regime and this solution has the same form as the Bunch-Davies vacuum,

$$u_{\mathbf{k}} = \begin{cases} C_1(k)z^* + C_2(k)z^* \displaystyle\int \frac{d\eta}{(z^*)^2}, & \text{if } k^2 \ll \dfrac{z^{*\prime\prime}}{z^*}. \\ \dfrac{\exp(ik\eta)}{\sqrt{2k}}, & \text{if } k^2 \gg \dfrac{z^{*\prime\prime}}{z^*}. \end{cases} \tag{4.43}$$

with C_1, and C_2 being complex integration constants. Note additionally that, super-horizon scales refer to wavelengths $\lambda \gg (aH)^{-1}$ or $k >> aH$, while sub-horizon scales refer to $\lambda \ll (aH)^{-1}$ or $k \ll aH$.

4.1 Numerical results

Our task in this section is to combine the theory and cosmological parameters. The inflationary parameters according with [Aghanim et al., 2018] are infered from Planck CMB observations of the power spectrum on a 68% confidence intervals for the base ΛCDM model, in combination with CMB lensing reconstruction and BAO.

n_s	0.9665 ± 0.0038
$\ln(10^{10}A_s)$	3.047 ± 0.014

Table 4.1: Inflation parameters

Since we already have found particular solutions for the background and perturbations, there are two things to take into account. First, we must set initial conditions for perturbations $u_{\mathbf{k}}$ evaluated at the end of inflation. Second, one could find the initial conditions for H_{end} and the vanishing pressure $P_{end} = 0$ with the observable curvature power spectrum $\mathcal{P}_\zeta(k)$ defined as,

$$\mathcal{P}_\zeta(k) = A_s \left(\frac{k}{k_0}\right)^{n_s - 1}. \tag{4.44}$$

With the typical value of the pivot scale set to $k_0 = 0.05 Mpc^{-1}$. In particular we assume this is valid towards the end of inflation due to this form (4.44) is always valid, buy only during inflation.
This represents the amplitude of the curvature perturbation on large scales $k \ll aH$ at the end of inflation (where the curvature perturbation is $\mathcal{R} \approx -\zeta$ on this scales). For a canonical single field inflation this also sets a scale for the perturbations produced,

$$\mathcal{P}_\zeta(k) = \left(\frac{H^2}{2\pi\dot{\phi}_0}\right)^2 \left(\frac{k}{aH}\right)^{3-2\nu_\phi}, \tag{4.45}$$

with the spectral index defined as,

$$n_s - 1 \equiv \frac{d\ln \mathcal{P}_\zeta(k)}{d\ln k} = 3 - 2\nu_\phi, \tag{4.46}$$

where in a slow-roll regime $\nu_\phi = \frac{3}{2} + 3\epsilon - \eta$.

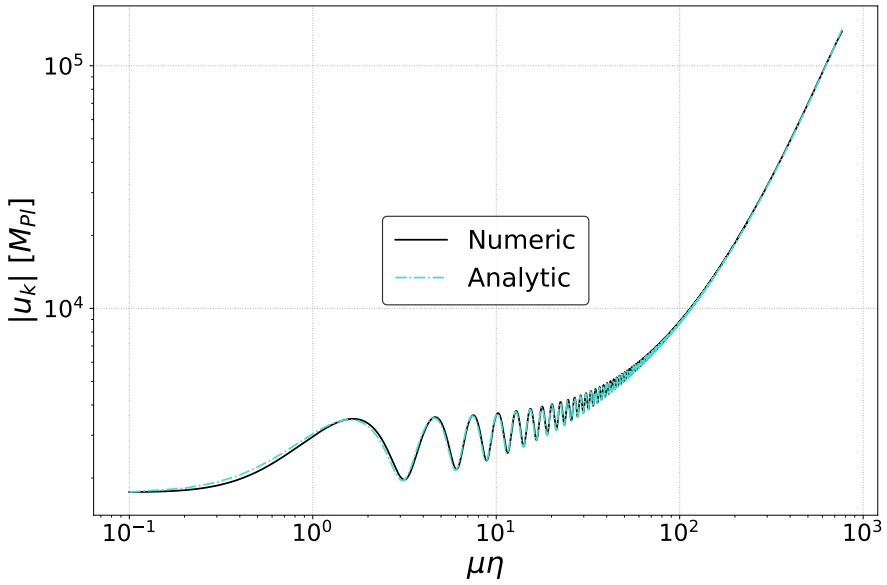

Figure 4.1: This is the comparison of both analytic (4.43) and numerical on the regime of $k^2 \ll z^{*\prime\prime}/z^*$, where we have used a soft matching and besides the initial conditions are chosen from the end of inflation.

The amplitude of modes at the end of inflation has been derived from [Bartolo et al., 2004]. According with them the solution at super-horizon and sub-horizon during inflation in terms of the M-S variable are given by,

$$u_{\mathbf{k}} = \begin{cases} \dfrac{aH}{\sqrt{2k^3}}\left(\dfrac{k}{aH}\right)^{-\nu_\phi+\frac{3}{2}} \exp(ik\eta) & \text{if } k^2 \ll \dfrac{z^{*\prime\prime}}{z^*} \\ \dfrac{\exp(ik\eta)}{\sqrt{2k}} & \text{if } k^2 \gg \dfrac{z^{*\prime\prime}}{z^*} \end{cases} \tag{4.47}$$

The above expressions are derived assuming that the scalar field drove from slow-roll approximation. For instance, if we evaluated in the particular case of

$k^2 \ll \frac{z^{*\prime\prime}}{z^*}$ at the end of inflation and then employing it as initial condition on (4.43) in the same regime, we find (see Figure 4.1) that the solution is consistent on both numerical and analytical cases at least.

Setup for numerical evolution

Actually, whether we match (4.44) and (4.45) at t_{end}, in order to obtain a value for H_{end} consistent with the observed power spectrum,

$$A_s \left(\frac{k}{k_0}\right)^{n_s-1} = \left(\frac{H_{end}^2}{2\pi\dot{\phi}_{end}}\right)^2 \left(\frac{k}{a_{end}\, H_{end}}\right)^{n_s-1}. \tag{4.48}$$

As a result of assuming a pressure-less background during Reheating, we find that,

$$A_s \left(\frac{1}{k_0}\right)^{n_s-1} = \left(\frac{H_{end}}{3\pi}\right)^2 \left(\frac{1}{a_{end}H_{end}}\right)^{n_s-1}. \tag{4.49}$$

$$H_{end} = (9\pi^2 A_s)^{1/(3-n_s)} \left(\frac{k_0}{a_{end}}\right)^{\frac{(1-n_s)}{(3-n_s)}}. \tag{4.50}$$

Using the values of Table 4.1, we have obtained a value of the order of,

$$H_{end} \sim 10^{-4} M_{Pl}. \tag{4.51}$$

As a consequence of this, let us mention that if this value is considered, then we are assuming that this scalar field must be the same field responsible for inflation, i.e. the inflaton. On the other hand, if the Reheating field ϕ is not the inflaton then the value of H_{end} is a free parameter for the initial conditions of our numerical evolution.
After setting initial conditions, we estimate the thermalization temperature or Reheating temperature T_r, which establishes the end of Reheating. A starting point comes from the density during Reheating, which we assume as pressure-less dust,

$$\rho_r = \frac{\pi}{30} g_* T_r^4 \propto a^{-3}. \tag{4.52}$$

Where g_* is the degrees of freedom. While oscillatory stage has values between $100 - 120$,

$$T_r = \left(\frac{30\rho_{end}}{\pi g_*}\right)^{\frac{1}{4}} \exp\left(-\frac{3N}{4}\right). \tag{4.53}$$

With N being the e-fold number elapsed from the end of inflation up to the end of Reheating. The Figure 4.2 is a contour plot of (4.53).
On the other hand, we need to computed a value of a_r the scale factor evaluated at moment of thermalization to employ it numerically. Furthermore, a_r must be subjected to T_r which has to be of the order of MeV in order to rethermalize the Universe in time for Big Bang Nucleosynthesis (BBN). However, [Kawasaki et al., 2000] reported constraints of $T_r > 4$ MeV $= 0.004$ GeV. With this in mind, we rescale the density from end of Reheating towards matter-radiation equality so,

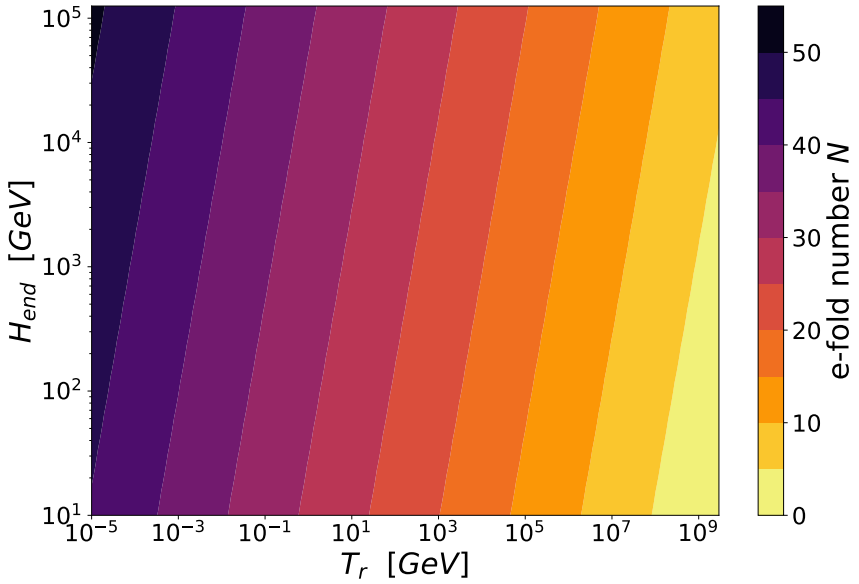

Figure 4.2: This plot shows the parameters-space and how parameters influence the values of the thermalization temperature T_r. So, on one hand slow Reheating occurs when T_r reaches low values. On the other hand the fast Reheating occurs when T_r reaches high values therefore, the e-fold number is reduced.

$$\rho_r = \rho_{eq}\left(\frac{a_{eq}}{a_r}\right)^4 = \frac{\pi}{30} g_* T_r^4. \tag{4.54}$$

$$\Rightarrow a_r = \left(\frac{30\rho_{eq}}{\pi g_*}\right)^{\frac{1}{4}}\left(\frac{a_{eq}}{T_r}\right). \tag{4.55}$$

Moreover after a few straightforward calculations, one could derive the next expression $\rho_{eq} = \frac{\Omega_{m,0}}{a_{eq}^3}\left(\frac{3H_0^2}{8\pi G}\right)$. For instance, according with Planck 2018 (see [Aghanim et al., 2018]), they inferred values of $H_0 = 67.5 \pm 0.5$ km/s/Mpc and $\Omega_{m,0} = 0.315 \pm 0.007$ and $z_{eq} \approx 3387$, whose base cosmological model was ΛCDM. Therefore, with the above at hand, we would calculate a value for (4.55).

Additionally, one look at the upper bound on the Reheating temperature T_r (see [Kofman, 1996]) which is $T_r < 10^9 GeV$. Nevertheless, Kofman argued that result is a very small temperature, at which the standard mechanism of baryogenesis in the GUTs cannot work.
In principle, we can look at a variety of Reheating scenarios by choosing values for the free parameters μ, H_{end} and N. For a given k-mode value and setting the free parameters consistent with the constraints, we have evolved the M-S variable following by (4.33) and employing (4.42).
Then we repeated this for a variety of k-modes around the instability scale (Jeans scale) depicted in Figure 4.3. The results are written in terms of the curvature and the matter perturbations as discussed below. In the rest of this thesis we show that some of the parameter space of them can be constrained from the bound to PBH abundance.

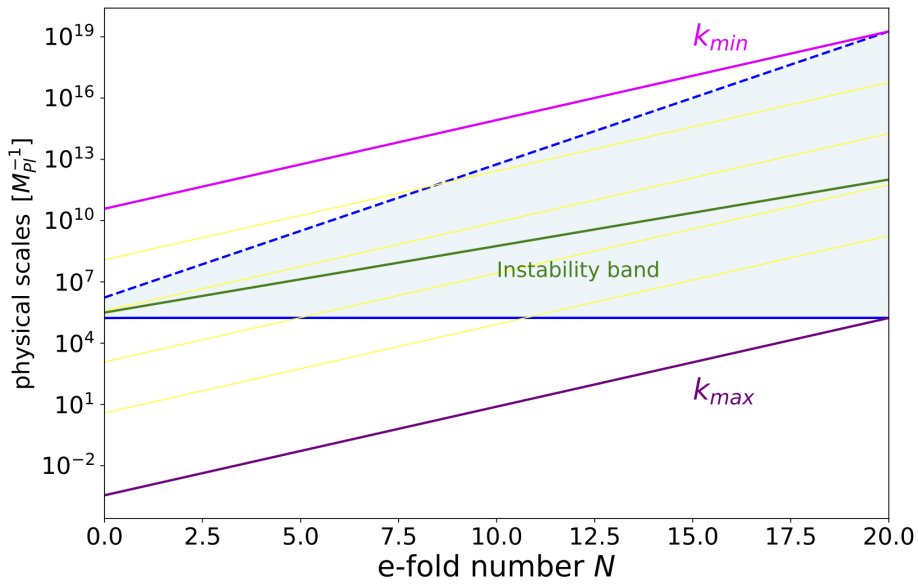

Figure 4.3: This plot is similar to that of [Jedamzik et al., 2010]. It shows the evolution of physical scales as function of the e-folds number through inflation and Reheating. In our case is considered during Reheating and for a complex scalar field. The upper bound in blue dashed lines is the Hubble horizon. The lower bound in blue continuous lines is the Jeans scale. The magenta line k_{min} represents a scale that crosses the Hubble horizon before the end of inflation and then reenters at the last e-fold or where we assumed that thermalization temperature T_r is reached. The purple line k_{max} is a scale that never exits the Hubble horizon but reaches the Jeans lenght only at the last e-fold of Reheating. The green is Mathieu's instability scale for the real case as discussed on Appendix A. The yellow lines just are the physical scales of different Fourier modes.

Primordial Curvature Power Spectrum

The curvature perturbation $\zeta_{\mathbf{k}}$ defined by (2.107) in terms of the M-S variable takes the following form,

$$\zeta_{\mathbf{k}} \equiv \frac{u_{\mathbf{k}}}{z}. \tag{4.56}$$

As long as this quantity is conserved on super-horizon scales, we can relate the power spectrum to the amplitude of the M-S variable at super-horizon scales during Reheating.

$$\mathcal{P}_\zeta = \frac{k^3}{2\pi}|\zeta_{\mathbf{k}}|^2. \tag{4.57}$$

In this Reheating scenario, the primordial power spectrum has a cut-off on the Planck scale[2] and also an upper limit at the scales which enter the horizon after thermalization has been reached (see Figure 4.4).

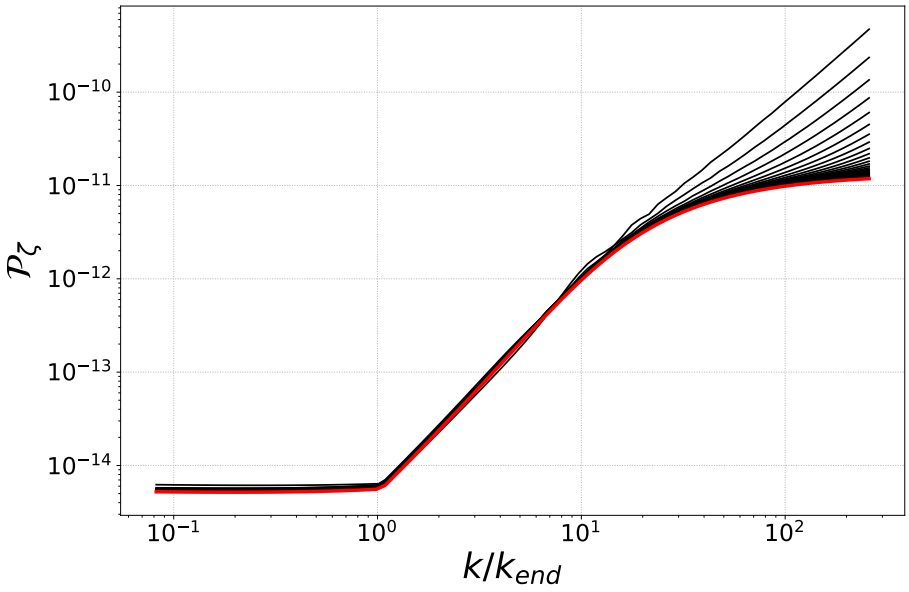

Figure 4.4: Primordial curvature power spectrum $\mathcal{P}_\zeta$ coming from PBHs versus wave number. For this plot we have used the inflation power spectrum as an initial condition.

Furthermore, notice that from our results one can look at Figure 4.4 that during inflation the curvature perturbation mode is constant on super-horizon scales $R' \simeq -\zeta' \simeq 0$.
In [Wands et al., 2000], they derived an expression for non-adiabatic perturbations given by,

$$\dot{\zeta} = -\frac{H}{\rho + P}\delta P_{nad}, \tag{4.58}$$

only valid on the uniform-density gauge and sufficiently large scales where gradient terms can be neglected. In terms of the conformal time,

[2]The cut-off to the power spectrum is introduced because scales below than the Planck scale cannot be adequately treated due to the emergence of quantum gravity effects.

$$\zeta' = -\frac{\mathcal{H}}{\rho + P}\delta P_{nad}. \tag{4.59}$$

As long as the pressure perturbation is completely adiabatic, implies that ζ is must be a constant at super-horizon scales as illustrated by our example.

4.2 Growth on matter fluctuations

Now we look at the growing mode on the case when k-modes are lower than Jeans wavenumber.

$$u_{\mathbf{k}} = C_1(k)z^* + C_2(k)\, z^* \int \frac{d\eta}{(z^*)^2}. \tag{4.60}$$

As a result of had a pressure-less background, it is acceptable to approximate $z(\eta)$ as $z(\eta) \approx a(\eta)$,

$$u_{\mathbf{k}} \approx C_1(k)a + C_2(k)\, a \int \frac{d\eta}{a^2}. \tag{4.61}$$

In accordance with Table 1.1, and using the relation (1.56),

$$\zeta_{\mathbf{k}} = C_1(k) - \frac{C_2(k)}{t}. \tag{4.62}$$

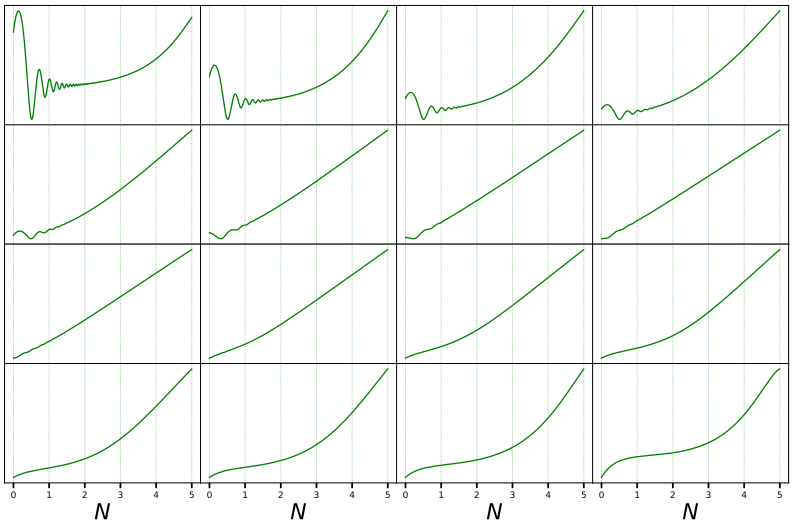

Figure 4.5: Shows the evolution of 16 modes chosen around the Jeans scale. The smaller wavenumbers do not grow significantly since they are above the horizon. they also are damped by oscillations. It is the middle range which grows most and in a power law as $\delta \sim a$.

The behavior of contrast density perturbation $\delta_{\mathbf{k}}$ defined by (2.10). Consequently, we may express $\delta_{\mathbf{k}}$ as a function of $\zeta_{\mathbf{k}}$ in this regime according with formula (2.116).

$$\delta_{\mathbf{k}} = -\frac{2}{5}\left(\frac{k^2}{a^2\, H^2} + 3\right)\zeta_{\mathbf{k}}. \tag{4.63}$$

The Bardeen potential is related to the quantity $\zeta_{\mathbf{k}}$ by (2.116). Then,

$$\delta_{\mathbf{k}} \approx -\frac{2}{5}\left(\frac{9k^2t^{\frac{2}{3}}}{4}+3\right)\left(C_1(k)-\frac{C_2(k)}{t}\right). \tag{4.64}$$

Therefore, in the case of large scales where $k >> 1$, the above expression can be reduced to,

$$\delta_{\mathbf{k}} \approx -\frac{9}{10}k^2\left(C_1(k)a - C_2(k)a^{-\frac{1}{2}}\right). \tag{4.65}$$

We just have found that $C_1(k)$ represents the growing mode and $C_2(k)$ the decay mode. Seeing that we are interested on the growth of perturbations, the decay mode $C_2(k)$ is neglected.
In the work of [Ballesteros et al., 2019] is discussed this particular regime. They agreed as well that the decay mode is determined by $C_2(k)$. As long as it decays sufficiently fast, the solution (4.60) quickly converges to $C_1(k)z^*$ and the amplitude of $C_1(k)$ can be obtained by matching with the short wavelength solutions. Although, this is not the way that we are assuming. This amplitude can be found in our case from matching the inflation solutions (4.47).
Keep in mind that the first term $C_1(k)$ is known the adiabatic mode that is conserved at super-horizon scales. On the other hand the second term $C_2(k)$ is the decaying mode which becomes negligible within a few e-folds after horizon crossing so that the constant mode is quickly reached.

Matter Power Spectrum

Likewise, the Power Spectrum of matter was computed, defined by,

$$\mathcal{P}_\delta = \frac{k^3}{2\pi}|\delta_{\mathbf{k}}|^2. \tag{4.66}$$

As it was shown in Figure 4.5, when perturbations are within Jeans instability band $\delta_{\mathbf{k}} \sim a$ and we then expect on particular scales,

$$\frac{\mathcal{P}_\delta(t_r)}{\mathcal{P}_\delta(t_{end})} = \frac{a_f^2}{a_{end}^2} = \exp(2N). \tag{4.67}$$

Furthermore the M-S variable can be related to the Bardeen potential. If we apply the Fourier transform as usual on (4.23),

$$\Psi_{\mathbf{k}} = -\frac{4\pi G\mathcal{H}}{a^2k^2}\left[z^2\left(\frac{u_{\mathbf{k}}^*}{z}\right)' + (z^*)^2\left(\frac{u_{\mathbf{k}}}{z^*}\right)'\right]. \tag{4.68}$$

Let us focus on first regime when $u_{\mathbf{k}} = C_1z^* + C_2z^*\int\frac{d\eta}{(z^*)^2}$. Thus, the Bardeen potential is,

$$\Psi_{\mathbf{k}} = -\frac{4\pi G\mathcal{H}}{a^2k^2}\left[C_2^* + C_2\right]. \tag{4.69}$$

Even though, on this regime the Bardeen potential might only have contributions by decay mode, this is an interesting result.

Now that we have obtained a growth in the amplitude of matter perturbations, we can assess the formation of PBHs and examine the cases where they are over-produced.

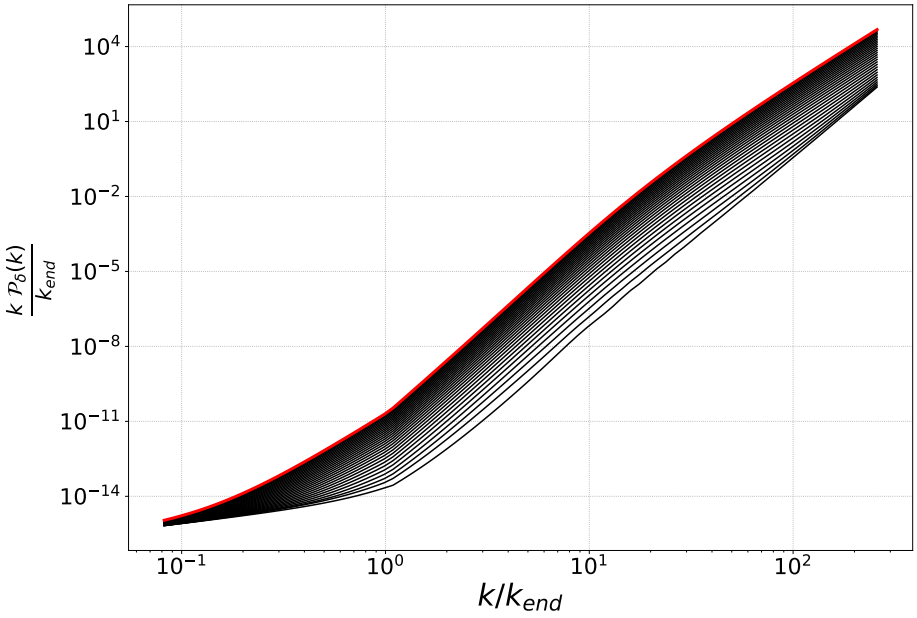

Figure 4.6: Evolution of Matter Power Spectrum during 5 e-folds. The red line is evaluated at t_r, that means the last e-fold.

4.3 PBH formation during Reheating

4.3.1 Primordial Black Holes

The simplest definition for a PBH is a peculiar type of black hole with a wide range of masses which is not formed as a result of a collapsed massive star known as stellar black holes, i.e. that mechanism is not subject to the well-known lower Chandrasekhar limit of $\sim 1.4 M_\odot$. For a review see [Carr, 2005].

If we compare the density of a black hole,

$$\rho_{BH} = 10^{18} \left(\frac{M}{M_\odot} \right)^{-2} \frac{g}{cm^3}, \tag{4.70}$$

and the cosmological density,

$$\rho_H = 10^{6} \left(\frac{t}{s} \right)^{-2} \frac{g}{cm^3}. \tag{4.71}$$

That means that how these perturbations could form PBHs from the direct collapse of matter clumps, it would have required a huge density in order to form small PBHs and that only could have been reached in early epochs.

Furthermore PBHs might be candidates of the black holes detected by The Laser Interferometer Gravitational-Wave Observatory (LIGO). The signal GW170729 [Abbott et al., 2019] with an estimated of 50^{+16}_{-10} and 34^{+9}_{-10} solar masses. These measurements do not coincide with usual stellar black holes mechanism and also spin absence is not usual coming from stars.

Sasaki argued in [Sasaki et al., 2018] that source of gravitational waves of binaries system could have been generated by PBHs. Additionally, accretion or merging of PBHs could explain the origin of Super Massive Black Holes with masses of $10^4 - 10^9 M_\odot$ located at the center of most galaxies or a novel characteristic of PBHs is that it may be the explanation of the supposed Planet 9 [Scholtz and Unwin, 2019] in our Solar System. If a black hole is ever observed with a mass significantly smaller than $< 1M_\odot$ will be an unequivocal proof of PBHs existence.

Formation criterion

In the standard mechanism, the cosmological density perturbations δ tend to collapse and this occurs according with Carr criterion (see [Carr, 1975] and [Harada et al., 2013]),

$$\alpha\lambda_J < R_{max} < \gamma R_H. \tag{4.72}$$

For some α and γ that encode the whole details of the collapse. Here R_H is Hubble horizon which encloses the density ρ_0, Jeans length λ_J and R_{max} is the size of the perturbation δ at the moment of a turn-around time in the spherical collapse model of structure formation. In the same model, this constraint can be written in terms of amplitudes of the density fluctuation δ, leading to a critical value of collapse. If the fluid presents an equation of state (1.55), then (4.72) can be expressed as,

$$\omega < \delta_{max} < 1. \tag{4.73}$$

Since our interest is on the collapse during a Reheating period when $\omega \approx 0$. The formation of PBHs is thus not limited to the critical value δ_c but by the time the spherical inhomogeneity takes to collapse. We adopt the criterion of considering an overdensity to collapse and form a PBH when it reaches the critical value of the spherical collapse model at $\delta_c = 1.68$.
Let us now look at how to compute the abundance of PBHs in a given cosmology. The variance $\sigma(R)$ is typically the size of fluctuations and is expressed as,

$$\sigma(R)^2 = \int_0^\infty W^2(kR)\mathcal{P}_\delta(k, t_{end})\frac{dk}{k}. \tag{4.74}$$

The probability distribution of the smoothed density contrast and $W(kR)$ is the Fourier transform of the window function used to smooth the density contrast. There is some freedom in the choice of $W(kR)$, and for simplicity, we set $W(kR)$ such that a Gaussian window function, for instance $W(kR) = \exp(-k^2R^2/2)$.

The primordial power spectrum has been constrained by assuming that it is scale invariant at each k, since the integral in $\sigma(R)^2$ is dominated by the scale $k = 1/R$. That is, for each scale k constrained by the abundance of PBHs with mass M_{PBH}.

According with Figure 4.7 we expected in some scales that,

$$\mathcal{P}_\delta(M, t) \sim \sigma(M, t)^2. \tag{4.75}$$

The initial abudance of PBH[3] with respect to the critical density is defined as,

[3]Some equations through this section have been taken from [Harada et al., 2016] and [Carr et al., 2018].

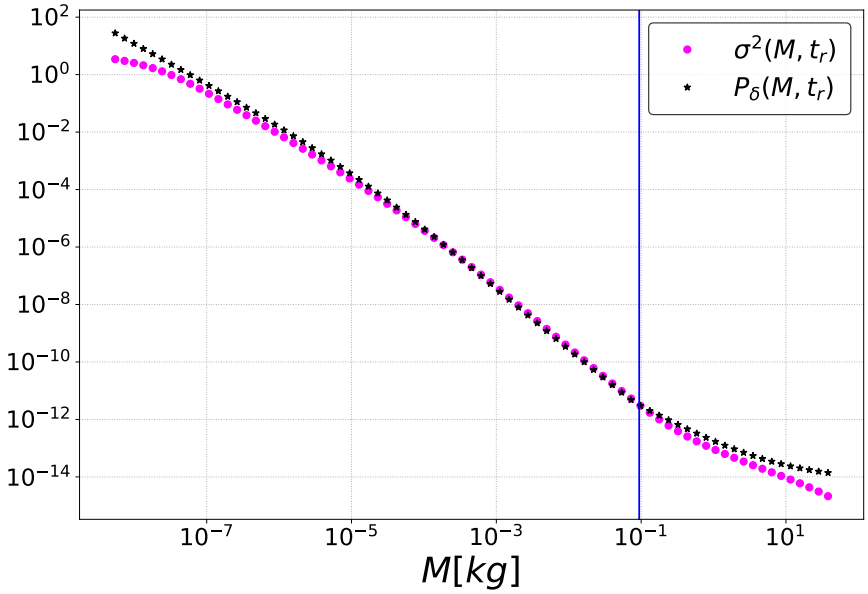

Figure 4.7: The vertical blue line represents the horizon mass evaluated at t_{end}.

$$\beta \equiv \frac{\rho_{PBH}}{\rho_c}. \tag{4.76}$$

Where ρ_{PBH} is density of PBHs. In accordance with Press-Schechter formalism, the abundance β of PBHs of mass M_{PBH} is equivalent to the probability that the smoothed density field exceeds the threshold δ_c as a result of spherical collapse. The fraction of the total energy density collapsing into PBHs of mass M is thus,

$$\beta(M) = 2\int_{\delta_c}^{\infty} \mathrm{P}(\delta)\, d\delta. \tag{4.77}$$

where $\mathrm{P}(\delta)$ is the probability distribution function (PDF) integrated with the adopted value $\delta_c = 1.68$ in a pressure-less scenario. Instead of expressing the horizon mass M_H in terms of radius $R = 1/k$, actually we prefer changing in terms of k-modes, so the horizon mass is given as,

$$M_H = \frac{4\pi(aR)^3\rho_0}{3}. \tag{4.78}$$

After substituting background expressions, we obtain that,

$$M_H = \frac{4\pi}{3}(aR)^3\rho_{end}\left(\frac{a_{end}}{a}\right)^3. \tag{4.79}$$

Reducing terms,

$$M_H = 4\pi R^3 H_{end}^2\, a_{end}^3. \tag{4.80}$$

Here we can rewrite as $k_{end} = a_{end}H_{end}$ and finding that,

$$M_H = \frac{4\pi}{H_{end}}\left(\frac{k_{end}}{k}\right)^3. \tag{4.81}$$

There are subtle assumptions that need to be taken into account. The first relevant assumption is the fact that the mass of PBHs is a fraction of the horizon mass, $M_{PBH} = \gamma M_H$, being γ the efficiency factor that encodes the details of the collapse. However, for simplicity we set γ to the unity. Second assumption is that initial perturbations have to be Gaussian, thus, the PDF of the smoothed density contrast is,

$$\mathrm{P}(\delta) = \frac{1}{\sqrt{2\pi}\sigma(M)} \exp\left(-\frac{\delta^2}{2\sigma(M)^2}\right). \tag{4.82}$$

Regardless of the way one choose the shape of PDF, the tail of this Gaussian PDF is related to the probability of forming a PBH of mass $> M$. Hence the assumption (4.82) allows us to change (4.77) into following formula,

$$\beta(M) = \mathrm{erfc}\left(\frac{\delta_c}{\sqrt{2}\,\sigma(M)}\right). \tag{4.83}$$

4.4 Cosmological constraints on the abundance of the PBHs

The abundance of PBHs is severely constrained by observations (see [Cangialosi, 2019], [Josan et al., 2009] and [Emami and Smoot, 2018]). Thus, the primordial curvature power spectrum as well and this fact has important implications on the formation of PBHs, since they could provide us with valuable information about the possible nature of dark matter, origin of non-stellar black holes and super massive black holes, Hawking radiation, among others. There are several number of limits spanning a wide range of masses values on the PBH abundance, we strongly recommend to see [Carr et al., 2010] and references therein.

The fact that PBHs might be small inspired Stephen Hawking to study their quantum features. This led to his famous discovery that black holes would thermally radiate like a black body radiation with an associated temperature,

$$T_{Hw} = \frac{1}{8\pi G M} \approx 10^{-7}\left(\frac{M}{M_\odot}\right) K. \tag{4.84}$$

It is better-know as *Hawking temperature*. As a result of this PBHs would evaporate on a timescale of,

$$\tau_{eva} = 1.90254 \times 10^{-34}\left(\frac{M}{\mathrm{g}}\right)^3 \text{ years}. \tag{4.85}$$

For instance, in an ideal case (where we are not considering accretion, merging and so forth) PBHs smaller than $M \sim 10^{15} g$ will have evaporated by the present epoch. So that means this process is too slow. This radiation has not been observationally confirmed so far.

If the black hole mass is decreasing due to Hawking radiation, thus the radius is too, and eventually reaches values close to ℓ_{Pl} Planck length. At that moment is speculated when the evaporation cease, the remanent are called a *Planck relic*.

Whatever be the cause of their stability, Planck relics would be a possible cold dark matter candidate. Indeed this leads to the Planck relics to be constrained. In particular, such relics could be left over from Reheating. If so, then relics may have a mass on the order of κ M_{Pl},

$$\beta(M) < 10^{-27}\kappa^{-1}\left(\frac{M}{M_{Pl}}\right)^{3/2}. \tag{4.86}$$

This is only valid for PBHs within the mass range[4],

$$1 < \frac{M}{M_{Pl}} < 10^{11}. \tag{4.87}$$

The upper mass limit arises because PBHs larger than this dominate the total density before they evaporate. Producing a critical density of relics obviously requires fine-tuning.
Observational constraints from (4.86) on PBHs abundance indicate that, for example, see Figure 4.8 if $\beta(M) < 10^{-20}$ translate into $\sigma^2(M) < 0.03333$ and therefore it might constrain the curvature power spectrum.

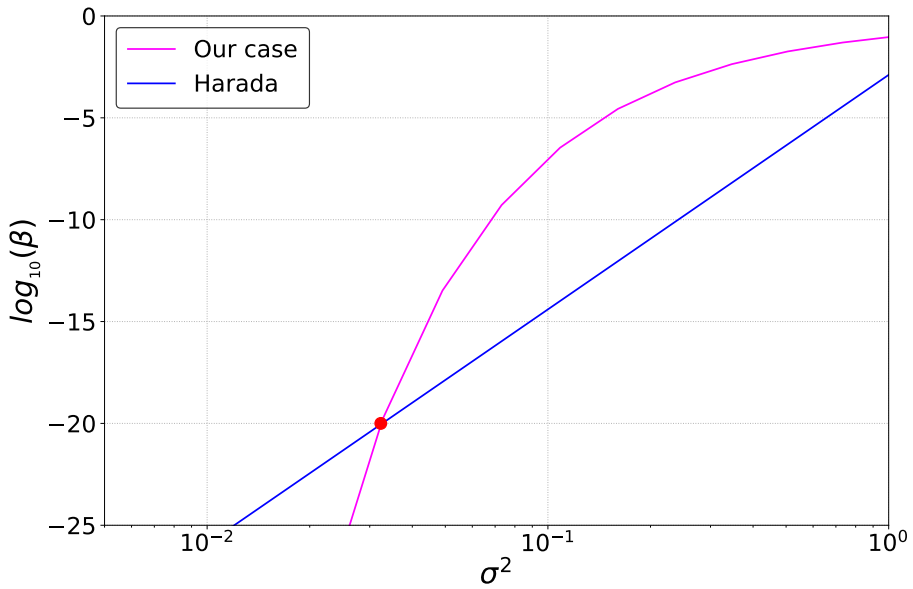

Figure 4.8: Following the evolution of $\sigma(M)$ evaluated at the moment of thermalization. This is also comparated with a semi-analytic formula $\beta = 0.05556\sigma^5$ found by [Harada et al., 2016].

Consequently, the specific parameters employed in this thesis, there is a range of values for which the constraint in (4.86) is violated. For example, in Figure 4.9 we show a few values of H_{end} that saturate the Planck relic constraint in Eq. (4.86), after considering the ratio $\mu/H_{end} = 10$ and in a period of Reheating that lapsed for $N = 5$ e-foldings.
On the other hand, fixing the scale at the end of inflation H_{end} and varying the e-folds number N we noticed that the constraint (4.86) is also violated from values $N > 2.8$ approximately. The direct consequence of this is inconsistency

[4]We also have assumed that Planck relics is approximated to M_{Pl}, i.e. the value of κ is set to unity.

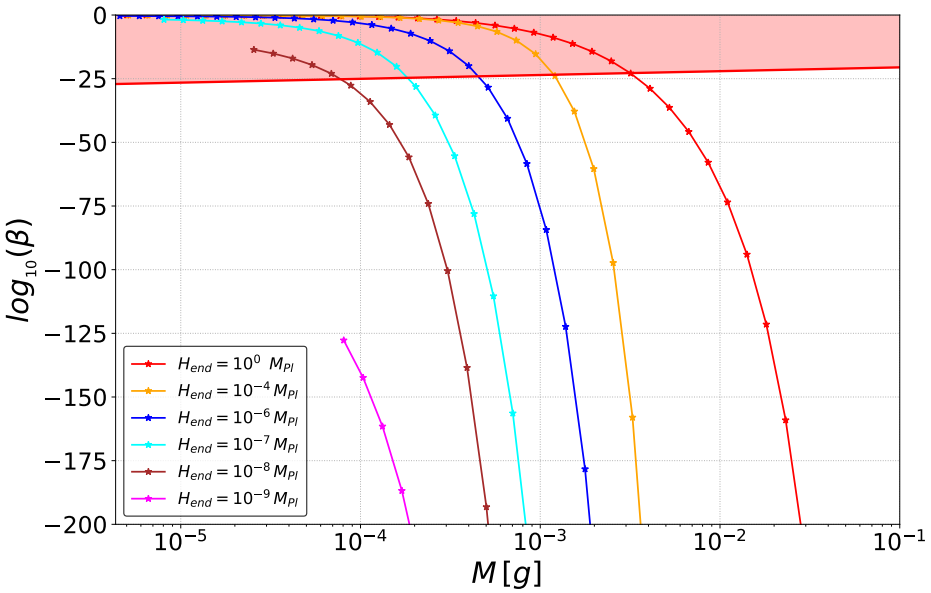

Figure 4.9: This plot was generated by setting e-fold number as $N = 5$ and varying the parameter H_{end} with a value of $\mu/H_{end} = 10$. The red-shaded region represents the values beyond the constraint given by Planck relics. Note that several models for the Reheating period violate the constraint on PBH abundance discussed in the text.

between the inhomogeneities produced during Reheating and the dark matter density observed if it was constituted by Planck-mass PBHs.

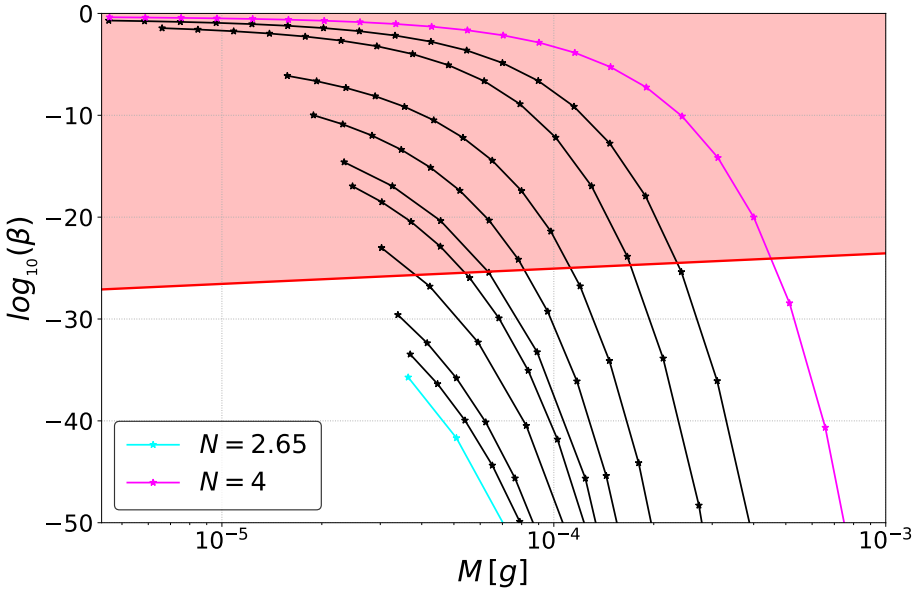

Figure 4.10: In this plot we fixed the values $H_{end} \approx 10^{-6}$ M$_{Pl}$ and the ratio $\mu/H_{end} = 10$, and varying values for several e-folds numbers.

Chapter 5

Conclusions and outlook

«The obvious is sometimes false; the unexpected is sometimes true»
Carl Sagan

In this thesis we discussed several features on the evolution of inhomogeneities of complex scalar field through harmonic potential model during Reheating.

Summary of results

Firstly of great relevance for our study, we found for the background that there are differences studying the real and complex cases in the fast oscillation regime $H \ll \mu$. In spite of this, both tend to a behavior of pressure-less fluid. This is shown in Figure A.1, even though, the biggest difference of them is the fact that real scalar field oscillates rapidly, and on average, it effectively behaves as pressure-less fluid, while the complex case does not present an oscillatory pressure. Reason which, motivated us to study the complex scalar field.

Subsequently, thanks to the use of the Mukhanov-Sasaki variable (4.21), we go on to find the equations that govern the perturbations of the complex scalar field, which were quite similar to those of the real scalar field. We noticed that expression (4.40) characterizes the Jeans scale in both cases is given purely by background quantities. Consequently with the background, we have obtained different analytical expressions for the real case given in (A.5) and complex in (4.42).

In the Figure 4.3, the instability band shows an ever-increasing range of wavenumbers, starting at the end of inflation; from the Jeans scale to the Hubble horizon, i.e. $k_H < k < k_J$, we realized that while the larger the ratio μ/H_{end} is, then the wider is the gap for instabilities.

After several calculations we found analytical solutions (4.43) which are valid in two different regimes and are also consistent with the numerical solutions to the M-S equation. Assuming that scalar field during Reheating must be the inflaton, we suggest initial conditions derived from the end of inflation and obey the slow-roll regime.

We proceed to analyze the statistic of these perturbations for different modes k defined in a range between $[k_{min}, k_{max}]$. We compute numerically the evolution of Matter Power Spectrum during $N = 5$ e-folds, concluding that within the

Jeans band there is a growth of such perturbations. As a result of the gravitational collapse of a scalar field it could have generated instabilities that emerged to form PBHs during Reheating.

Then, in order to compute the abundance of PBHs $\beta(M)$ from collapse of scalar field density perturbations, we look for initially density perturbations on certain scales which were substantially entering towards Jeans instability band or they already were in the band. We noticed that, at these scales, pertubations grow as the scale factor $\delta_{\mathbf{k}} \propto a$. This is the behavior we were looking for, because, is the form of growing mode in the dust perturbations at linear order that lead to structure formation.

Nevertheless, it is important to mention that the formation of PBHs had been conventionally studied in the radiation-dominated epoch, considering the fact that δ_c on this scenario has a threshold of $\delta_c = 0.47$ until recently [Harada et al., 2016] (see also [Niemeyer and Easther, 2019]). In this thesis the scalar field was studied through an epoch of matter-dominated, until the end of Reheating with a different threshold of $\delta_c = 1.68$ as result of the well-known spherical collapse by dust. Radiation-domination begins when the M mass of PBHs are formed otherwise the β values would be too high.

One of the currently hypothesis (and perhaps the right one) is the fact that dark matter could be composed of PBHs, based on at its low masses would behaves as expected of other particles candidates for dark matter. Planck-mass relics could make up the Dark Matter today, if they are stable relics. In order not to exceed the current observed CDM density, there would be an upper limit on the abundance of the PBHs.

Ultimately, another case in which this situation could occur is when ϕ was not the inflaton but still can reheat the Universe, such that, initial conditions have to be changed, constraining the free parameters of this independent Reheating model as presented even more.

Soon the next generation of observations will have the challenge of measuring the B modes of the CMB with higher resolution than Planck. In order to help us scrapping out inflationary models and getting a better understanding of the post-inflationary stage. Or perhaps provide a definitive clue or hint for the explanation of the Reheating phase.

Future perspectives

To put things into perspective, the results presented might give way to obtain analytical approaches for the growth of δ which are valid only on small scales and therefore on power spectrum too. Also, it is possible to approximate $\beta(M)$ analytically, in order to test Reheating models analytically as well. According with Figure 4.5 in certain regions $\delta_{\mathbf{k}} \propto a$ and further Figure 4.7 we may expect,

$$\mathcal{P}_\delta(M,t) \propto \sigma(M,t)^2 \propto |\delta_{\mathbf{k}}|^2 \propto a^2. \tag{5.1}$$

For instance, there are scenarios that find an overproduction of PBHs. And these could be discarded or rejected by analytical approaches.

Possible extensions of this thesis

A few extensions to the present work are in sight, some of which are listed below:

- ⋆ Consider more involved models of Reheating includying, e.g. self-interacting potentials (see [Amin et al., 2015]). This would lead to a new set of scenarios to be constrained by the abundance of PBHs produced during this period. Another possibility is to consider more than one scalar field in order to address phenomena arising in more realistic preheating models.
- ⋆ Considering the complete inflation model (e.g. [Mishra and Sahni, 2019]), it is possible to constrain the primordial powerspectrum with the bounds to the PBH abundance reported here. Changing the prescriptions to the primordial powerspectrum at small scales (so far unobserved), its parameters could be constrained with the same analysis here presented.
- ⋆ With the solutions obtained at first order, it is possible to set semi-analytic inital conditions to the non-linear gravitational collapse, and subsequent black hole formation. It remains to look at the compatibility with linear solutions to the ADM system in Eqs.(2.122) to (2.128), and subsequently motivate to run simulations of PBH formation looking at critical values for the collapse of the cosmological scalar field.

Appendices

Appendix A

Real case

On this Appendix we would like to examine and discuss the real scalar field. As we have found in Section 3.1, for the background the solution of real case is given by (3.23).

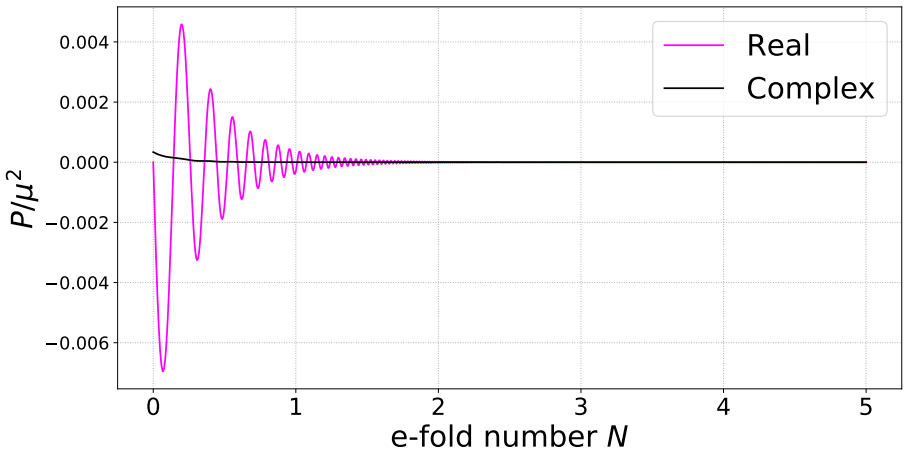

Figure A.1: Numerically the pressure for both cases, as a function of e-folds number.

Moreover indicated from previous Figure A.1 (also see [Hidalgo et al., 2017]), when we average solution (3.23) over a single period of oscillation $1/\mu$, implies that,

$$\langle \rho \rangle = \frac{1}{2}\langle \Pi^2 \rangle + \frac{1}{2}\mu^2 \langle \phi^2 \rangle \approx \mu^2 \langle \phi^2 \rangle \approx \frac{\mu^2 \phi_0^2}{2} a^{-3} + \mathcal{O}^2\left(\frac{H}{\mu}\right). \tag{A.1}$$

$$\langle P \rangle = \frac{1}{2}\langle \Pi^2 \rangle - \frac{1}{2}\mu^2 \langle \phi^2 \rangle \approx \frac{9\phi_0^2 H^2}{16 a^3} \approx 0. \tag{A.2}$$

As a result of this behavior, if the oscillating scalar field dominates the Universe for sufficiently long time, it effectively behaves as pressure-less fluid.

Through of the perturbative regime on the real case, and employing the M-S variable (4.21), leads to the following equation,

$$u_{\mathbf{k}}'' + \left(k^2 - \frac{z''}{z}\right) u_{\mathbf{k}} = 0. \tag{A.3}$$

In the case when $k^2 \ll z''/z$, the solution is,

$$u_{\mathbf{k}} = C_1(k)z + C_2(k)\, z \int \frac{d\eta}{z^2}. \tag{A.4}$$

with $C_1(k)$ and $C_2(k)$ integration constants which must be determined, as usual, from the Bunch-Davies vacuum solution.
Notice from Figure 3.1 and A.1 that real scalar field holds closely of standard CDM scenario with small oscillations around it. Thus, expression (4.34) can be simplified by making use of background equations with an explicit instability scale in the evolution. According with [Alcubierre et al., 2015],

$$\frac{z''}{z} \approx -\mu^2 a^2 \left[1 - 6\left(\frac{H}{\mu}\right)\sin(2\mu t) + \mathcal{O}^2\left(\frac{H}{\mu}\right)\right]. \tag{A.5}$$

Where we have done a new change of variable $x \equiv \mu t + \pi/4$ on A.3 and one would obtain the Mathieu equation as follow,

$$\frac{d^2 u_{\mathbf{k}}}{dx^2} + [A(\mathbf{k}) - 2q\cos(2x)]\, u_{\mathbf{k}} = 0. \tag{A.6}$$

where $A(\mathbf{k}) = 1 + \dfrac{k^2}{\mu^2\, a^2}$ and $q = 3\dfrac{H}{\mu} + \mathcal{O}^2\left(\dfrac{H}{\mu}\right)$.

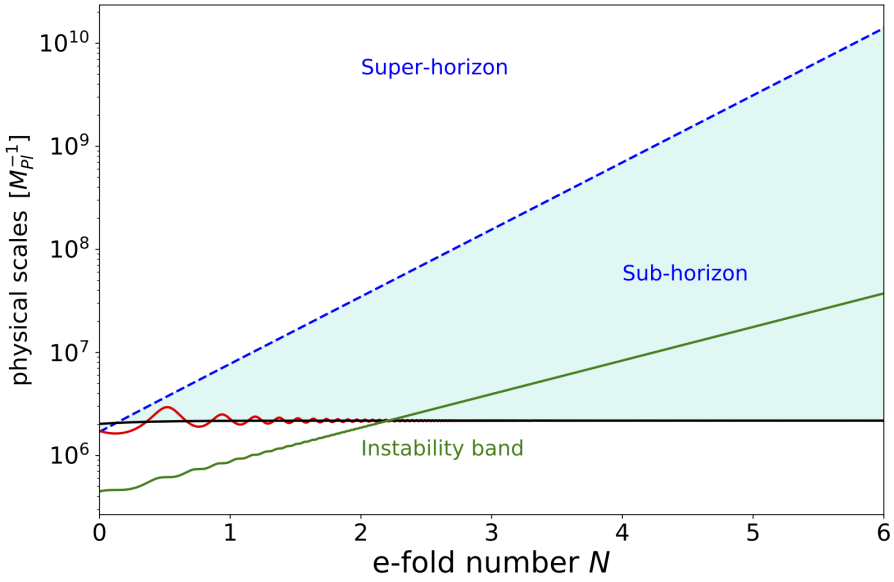

Figure A.2: The teal-shaded region is delimited by Horizon scales and Jeans scales. Nevertheless, there are several regions which are restricted by Mathieu's instability scale. For example the region between Mathieu's and Jeans scale.

As we saw on large scales (for instance, CMB scales), the conservation of curvature perturbation is sufficient to establish that the power spectrum calculated at the end of inflation propagates through the Reheating epoch without being distorted. Since $q \ll 1$, we are in the narrow resonance regime. According with [Jedamzik et al., 2010] the first instability band is given by,

$$1 - q < A_{\mathbf{k}} < 1 + q, \tag{A.7}$$

Therefore,

$$0 < k < a\sqrt{3H\mu}, \tag{A.8}$$

the new characteristic spatial length given by $R_c \equiv 1/\sqrt{3H\mu}$, which sets the lower bound of the instability band (see Figure (A.2)), the oscillations source a parametric resonance. Fortunately, thanks to these oscillations (A.3) becomes into Mathieu equation with an instability band of that equation.

Bibliography

Abbott, B. P. et al. (2016). Observation of Gravitational Waves from a Binary Black Hole Merger. *Phys. Rev. Lett.*, 116(6):061102.

Abbott, B. P. et al. (2017). GW170104: Observation of a 50-Solar-Mass Binary Black Hole Coalescence at Redshift 0.2. *Phys. Rev. Lett.*, 118(22):221101.

Abbott, B. P. et al. (2019). GWTC-1: A Gravitational-Wave Transient Catalog of Compact Binary Mergers Observed by LIGO and Virgo during the First and Second Observing Runs. *Phys. Rev.*, X9(3):031040.

Aghanim, N. et al. (2018). Planck 2018 results. VI. Cosmological parameters.

Akiyama, K. et al. (2019). First M87 Event Horizon Telescope Results. I. The Shadow of the Supermassive Black Hole. *Astrophys. J.*, 875(1):L1.

Alcubierre, M., de la Macorra, A., Diez-Tejedor, A., and Torres, J. M. (2015). Cosmological scalar field perturbations can grow. *Physical Review D*, 92(6):063508.

Amin, M. A., Hertzberg, M. P., Kaiser, D. I., and Karouby, J. (2015). Nonperturbative dynamics of reheating after inflation: a review. *International Journal of Modern Physics D*, 24(01):1530003.

André, P., Baccigalupi, C., Banday, A., Barbosa, D., Barreiro, B., Bartlett, J., Bartolo, N., Battistelli, E., Battye, R., Bendo, G., et al. (2014). Prism (polarized radiation imaging and spectroscopy mission): an extended white paper. *Journal of Cosmology and Astroparticle Physics*, 2014(02):006.

Ballesteros, G., Jiménez, J. B., and Pieroni, M. (2019). Black hole formation from a general quadratic action for inflationary primordial fluctuations. *Journal of Cosmology and Astroparticle Physics*, 2019(06):016.

Bardeen, J. M. (1980). Gauge Invariant Cosmological Perturbations. *Phys. Rev.*, D22:1882–1905.

Bartolo, N., Komatsu, E., Matarrese, S., and Riotto, A. (2004). Non-gaussianity from inflation: Theory and observations. *Physics Reports*, 402(3-4):103–266.

Baumann, D. (2012). Cosmology. *Part III Mathematical Tripos*.

Cangialosi, A. (2019). Cosmological constraints on primordial black holes.

Carr, B., Dimopoulos, K., Owen, C., and Tenkanen, T. (2018). Primordial Black Hole Formation During Slow Reheating After Inflation. *Phys. Rev.*, D97(12):123535.

Carr, B. J. (1975). The primordial black hole mass spectrum. , 201:1–19.

Carr, B. J. (2005). Primordial Black Holes: Do They Exist and Are They Useful? *arXiv e-prints*, pages astro–ph/0511743.

Carr, B. J., Kohri, K., Sendouda, Y., and Yokoyama, J. (2010). New cosmological constraints on primordial black holes. *Phys. Rev.*, D81:104019.

Carroll, S. M. (2004). *Spacetime and geometry: An introduction to general relativity*.

Cedeño, F. X. L., González-Morales, A. X., and Ureña-López, L. A. (2017). Cosmological signatures of ultralight dark matter with an axionlike potential. *Phys. Rev.*, D96(6):061301.

Delabrouille, J. et al. (2018). Exploring cosmic origins with CORE: Survey requirements and mission design. *JCAP*, 1804(04):014.

Dodelson, S. (2003). *Modern cosmology*. Elsevier.

Einstein, A. (1915). Die Feldgleichungen der Gravitation. *Sitzungsberichte der Königlich Preußischen Akademie der Wissenschaften (Berlin), Seite 844-847*.

Ellis, G. F., Maartens, R., and MacCallum, M. A. (2012). *Relativistic cosmology*. Cambridge University Press.

Emami, R. and Smoot, G. F. (2018). Observational constraints on the primordial curvature power spectrum. *Journal of Cosmology and Astroparticle Physics*, 2018(01):007.

Eötvös, L. (2008). On the gravitation produced by the earth on different substances. *Abraham Zelmanov J*, 1(6).

Frolov, A. V. (2010). Nonlinear dynamics and primordial curvature perturbations from preheating. *Classical and Quantum Gravity*, 27(12):124006.

Garcıa-Bellido, J. Inflation and reheating.

Guth, A. H. (1981). Inflationary universe: A possible solution to the horizon and flatness problems. *Physical Review D*, 23(2):347.

Harada, T., Yoo, C.-M., and Kohri, K. (2013). Threshold of primordial black hole formation. *Phys. Rev.*, D88(8):084051. [Erratum: Phys. Rev.D89,no.2,029903(2014)].

Harada, T., Yoo, C.-m., Kohri, K., Nakao, K.-i., and Jhingan, S. (2016). Primordial black hole formation in the matter-dominated phase of the universe. *The Astrophysical Journal*, 833(1):61.

Hartle, J. B. (2003). *Gravity: An introduction to Einstein's general relativity*. AAPT.

Hazumi, M., Ade, P., Akiba, Y., Alonso, D., Arnold, K., Aumont, J., Baccigalupi, C., Barron, D., Basak, S., Beckman, S., et al. (2019). Litebird: A satellite for the studies of b-mode polarization and inflation from cosmic background radiation detection. *Journal of Low Temperature Physics*, 194(5-6):443–452.

Hidalgo, J. C., De Santiago, J., German, G., Barbosa-Cendejas, N., and Ruiz-Luna, W. (2017). Collapse threshold for a cosmological Klein Gordon field. *Phys. Rev.*, D96(6):063504.

Jedamzik, K., Lemoine, M., and Martin, J. (2010). Collapse of Small-Scale Density Perturbations during Preheating in Single Field Inflation. *JCAP*, 1009:034.

Jetzer, P. and Scialom, D. (1997). Time evolution of the perturbations for a complex scalar field in Friedmann-Lemaitre universe. *Phys. Rev.*, D55:7440–7450.

Josan, A. S., Green, A. M., and Malik, K. A. (2009). Generalised constraints on the curvature perturbation from primordial black holes. *Phys. Rev.*, D79:103520.

Kawasaki, M., Kohri, K., and Sugiyama, N. (2000). Mev-scale reheating temperature and thermalization of the neutrino background. *Physical Review D*, 62(2).

Kirklin, J. (2015). Cosmology. *Based on a course given by James Fergusson and David Marsh. Cambridge Part III Maths*.

Kofman, L., Linde, A. D., and Starobinsky, A. A. (1994). Reheating after inflation. *Phys. Rev. Lett.*, 73:3195–3198.

Kofman, L. A. (1996). The Origin of matter in the universe: Reheating after inflation.

Kogut, A., Fixsen, D., Chuss, D., Dotson, J., Dwek, E., Halpern, M., Hinshaw, G., Meyer, S., Moseley, S., Seiffert, M., et al. (2011). The primordial inflation explorer (pixie): a nulling polarimeter for cosmic microwave background observations. *Journal of Cosmology and Astroparticle Physics*, 2011(07):025.

Lachièze-Rey, M. (2012). *Theoretical and observational cosmology*, volume 541. Springer Science & Business Media.

Liddle, A. R., Parsons, P., and Barrow, J. D. (1994). Formalizing the slow roll approximation in inflation. *Phys. Rev.*, D50:7222–7232.

Linde, A. D. (1984). The inflationary universe. *Reports on Progress in Physics*, 47(8):925.

Lyth, D. H. and Liddle, A. R. (2009). *The primordial density perturbation: Cosmology, inflation and the origin of structure*. Cambridge University Press.

Malik, K. A. and Wands, D. (2009). Cosmological perturbations. *Phys. Rept.*, 475:1–51.

Martin, J. (2004). Inflation and precision cosmology. *Brazilian journal of physics*, 34(4A):1307–1321.

Martin, J., Papanikolaou, T., and Vennin, V. (2019). Primordial black holes from the preheating instability. *arXiv preprint arXiv:1907.04236*.

Matos, T., Luevano, J.-R., Quiros, I., Urena-Lopez, L. A., and Vazquez, J. A. (2009). Dynamics of scalar field dark matter with a cosh-like potential. *Physical Review D*, 80(12):123521.

Matos, T. and Urena-Lopez, L. A. (2000). Quintessence and scalar dark matter in the universe. *Class. Quant. Grav.*, 17:L75–L81.

Mishra, S. S. and Sahni, V. (2019). Primordial black holes from a tiny bump in the inflaton potential. *arXiv preprint arXiv:1911.00057*.

Misner, C. W., Thorne, K. S., and Wheeler, J. A. (2017). *Gravitation*. Princeton University Press.

Niemeyer, J. C. and Easther, R. (2019). Inflaton Clusters and Inflaton Stars.

Peter, P. and Uzan, J.-P. (2013). *Primordial cosmology*. Oxford University Press.

Poisson, E. (2002). *An advanced course in general relativity*.

Riess, A. G. (2019). The expansion of the universe is faster than expected. *Nature Reviews Physics*, pages 1–3.

Sasaki, M., Suyama, T., Tanaka, T., and Yokoyama, S. (2018). Primordial black holes—perspectives in gravitational wave astronomy. *Class. Quant. Grav.*, 35(6):063001.

Scholtz, J. and Unwin, J. (2019). What if Planet 9 is a Primordial Black Hole?

Schutz, B. (2009). *A first course in general relativity*. Cambridge university press.

Spergel, D. N. (2015). The dark side of cosmology: Dark matter and dark energy. *Science*, 347(6226):1100–1102.

Torres, J. M., Alcubierre, M., Diez-Tejedor, A., and Núñez, D. (2014). Cosmological nonlinear structure formation in full general relativity. *Phys. Rev. D*, 90:123002.

Torres-Lomas, E., Hidalgo, J. C., Malik, K. A., and Ureña-López, L. A. (2014). Formation of subhorizon black holes from preheating. *Phys. Rev.*, D89(8):083008.

Tsujikawa, S. (2013). Quintessence: a review. *Classical and Quantum Gravity*, 30(21):214003.

Wands, D., Malik, K. A., Lyth, D. H., and Liddle, A. R. (2000). A New approach to the evolution of cosmological perturbations on large scales. *Phys. Rev.*, D62:043527.